

**UNCLASSIFIED**

**AD 428230**

**DEFENSE DOCUMENTATION CENTER**

**FOR**

**SCIENTIFIC AND TECHNICAL INFORMATION**

**CAMERON STATION, ALEXANDRIA, VIRGINIA**



**UNCLASSIFIED**

NOTICE: When government or other drawings, specifications or other data are used for any purpose other than in connection with a definitely related government procurement operation, the U. S. Government thereby incurs no responsibility, nor any obligation whatsoever; and the fact that the Government may have formulated, furnished, or in any way supplied the said drawings, specifications, or other data is not to be regarded by implication or otherwise as in any manner licensing the holder or any other person or corporation, or conveying any rights or permission to manufacture, use or sell any patented invention that may in any way be related thereto.

N-64-8

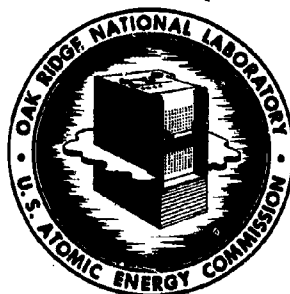
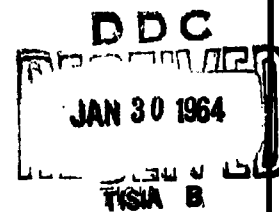
188

CATALOGED BY DDC  
428230  
AS AD No. \_\_\_\_\_

ORNL-3464  
UC-34 - Physics  
TID-4500 (24th ed.)

A STUDY OF THE RADIATION SHIELDING  
CHARACTERISTICS OF BASIC CONCRETE  
STRUCTURES AT THE TOWER  
SHIELDING FACILITY

V. R. Cain



**OAK RIDGE NATIONAL LABORATORY**  
operated by  
**UNION CARBIDE CORPORATION**  
for the  
**U.S. ATOMIC ENERGY COMMISSION**

428230

Printed in USA. Price: \$1.75 Available from the  
Office of Technical Services  
U. S. Department of Commerce  
Washington 25, D. C.

#### LEGAL NOTICE

This report was prepared as an account of Government sponsored work. Neither the United States, nor the Commission, nor any person acting on behalf of the Commission:

A. Makes any warranty or representation, expressed or implied, with respect to the accuracy, completeness, or usefulness of the information contained in this report, or that the use of any information, apparatus, method, or process disclosed in this report may not infringe privately owned rights; or

B. Assumes any liabilities with respect to the use of, or for damages resulting from the use of any information, apparatus, method, or process disclosed in this report.

As used in the above, "person acting on behalf of the Commission" includes any employee or contractor of the Commission, or employee of such contractor, to the extent that such employee or contractor of the Commission, or employee of such contractor prepares, disseminates, or provides access to, any information pursuant to his employment or contract with the Commission, or his employment with such contractor.

#### DDC AVAILABILITY NOTICE

Qualified requestors may obtain copies of this report from the Defense Documentation Center, Arlington Hall Station, Arlington, Virginia.

Contract No. W-7405-eng-26

Neutron Physics Division

A STUDY OF THE RADIATION SHIELDING CHARACTERISTICS OF BASIC  
CONCRETE STRUCTURES AT THE TOWER SHIELDING FACILITY\*

V. R. Cain

Date Issued

JAN 21 1964

OCD Review Notice

This report has been reviewed in the Office of Civil Defense and approved for publication. Approval does not signify that the contents necessarily reflect the views and policies of the Office of Civil Defense.

\*Work supported under Contract OCD-OS-62-145.

OAK RIDGE NATIONAL LABORATORY  
Oak Ridge, Tennessee  
operated by  
UNION CARBIDE CORPORATION  
for the  
U. S. ATOMIC ENERGY COMMISSION

# ABSTRACT

In the first of a series of experiments performed for the Department of Defense to investigate the protection afforded by various typical structures against prompt weapons radiation, radiation-intensity measurements were made at the Tower Shielding Facility in two concrete-shielded bunkers and in an interconnecting tunnel. Prompt weapons radiation was simulated by the Tower Shielding Reactor II (TSR-II), which was operated 100 ft above the ground. The distance between the reactor and the bunkers was approximately 700 ft. The bunkers were each 12-ft cubes and were constructed so that the shield thickness on the front face of one and on the top face of the other could be varied in 4-in. steps from 0 to 20 in. The thickness of concrete and dirt surrounding all other faces was sufficient to make them black to incident radiation.

The immediate goals of the experiment were to study (1) the attenuation of radiations by various thicknesses of ordinary concrete slabs, (2) the buildup of radiation intensities within the cavities by scattering of radiation in the walls, and (3) the transmission of radiation down a tunnel with two right-angle bends. The gamma-ray and fast-neutron dose rates and thermal-neutron fluxes measured at various positions within the bunkers and in the tunnel and the pulse-height spectra from a 3-in. sodium iodide crystal determined at one position in the top bunker and one position in the tunnel are reported.

iv  
TABLE OF CONTENTS

	<u>Page No.</u>
Abstract -----	iii
Introduction -----	1
Facility Description -----	1
Bunker Description -----	4
Instrument Description -----	8
Dose-Rate and Flux Measurements in Bunkers -----	11
Dose-Rate and Flux Measurements in Tunnel -----	23
Gamma-Ray Spectra Determinations -----	24
List of Figures -----	60

Best Available Copy

## INTRODUCTION

A research program is being undertaken at Oak Ridge National Laboratory with the ultimate goal of producing simplified calculational methods for estimating the protection afforded by various typical structures against prompt weapons radiation. The first experiment in this program was carried out at the Tower Shielding Facility in consultation and cooperation with the Department of Defense, Office of Civil Defense, and consisted of radiation-intensity measurements in two concrete-shielded bunkers and an interconnecting tunnel. Prompt weapons radiation was simulated by the Tower Shielding Reactor II (TSR-II), which was operated 100 ft above the ground. The distance between the reactor and the bunkers was approximately 700 ft.

The immediate goals of the experiment were (1) to study the attenuation of radiations by various thicknesses of ordinary concrete slabs, (2) to investigate the buildup of radiation intensities within the structure by scattering of radiation in the walls, and (3) to study the transmission of radiation down a tunnel with two right-angle bends. This report describes the experiment and presents the results. An analysis of the data will be given in a subsequent report to be submitted to the Defense Atomic Support Agency (DASA).

## FACILITY DESCRIPTION

The Tower Shielding Facility consists of four 315-ft towers which support the TSR-II and other experimental equipment at heights as high as 200 ft. Each tower is located at the corner of a 100 by 200 ft rectangle, with the TSR-II suspended between towers I and II as shown in Figs. 1 and 2. For this experiment no other equipment was suspended from the structure.

The TSR-II is a water-moderated and -cooled reactor constructed of MTR-type fuel plates which form a spherical annulus.<sup>1</sup> The entire assembly

1. L. B. Holland and C. E. Clifford, Description of the Tower Shielding Reactor II and Proposed Preliminary Experiments, ORNL-2747 (1959); L. B. Holland et al., Neutron Phys. Div. Ann. Prog. Rep. Sept. 1, 1959, ORNL-2842, p. 39; L. B. Holland et al., Neutron Phys. Div. Ann. Prog. Rep. Sept. 1, 1960, ORNL-3016, p. 42.



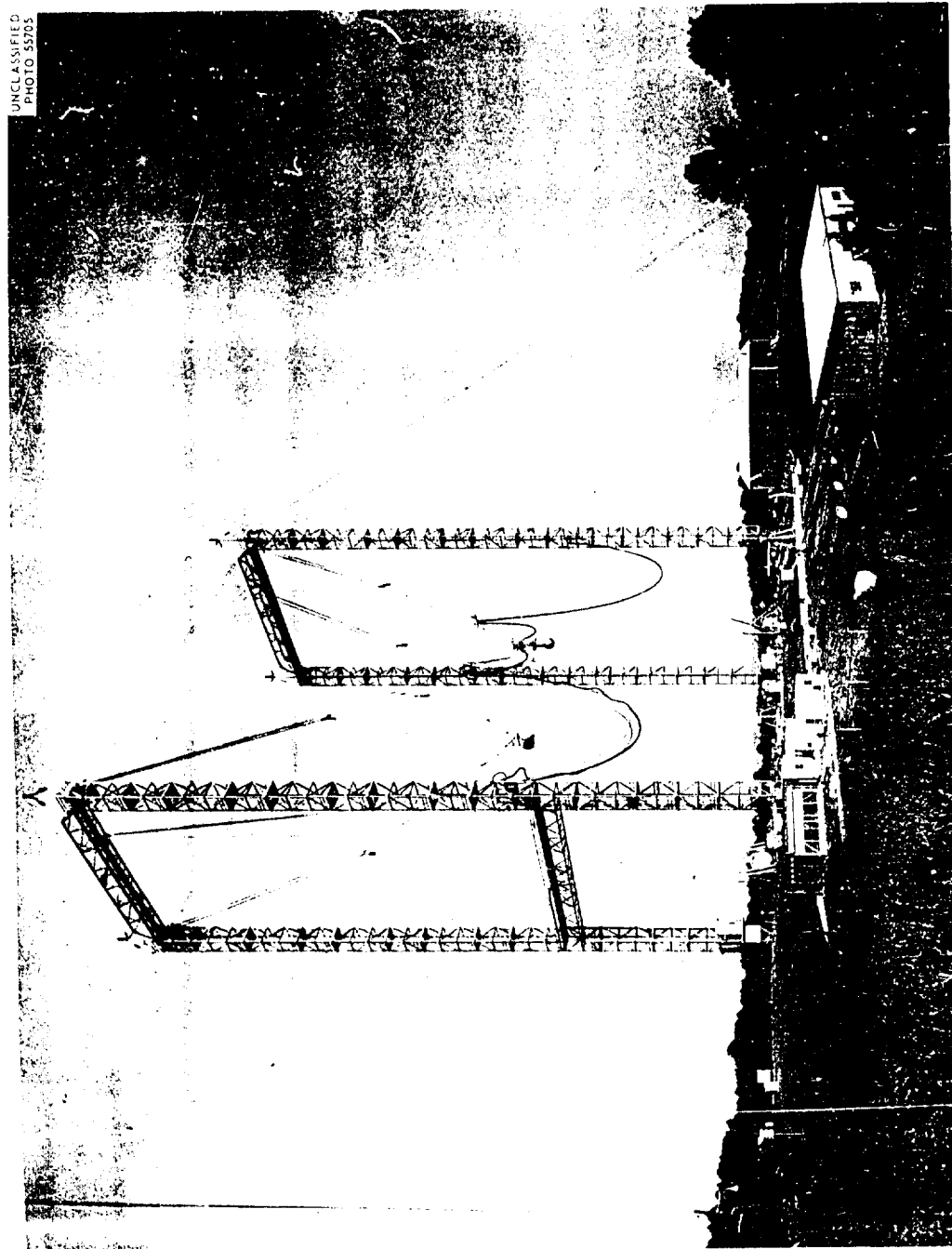


Fig. 1. Tower Shielding Facility.

UNCLASSIFIED  
2-01-056-039-1417

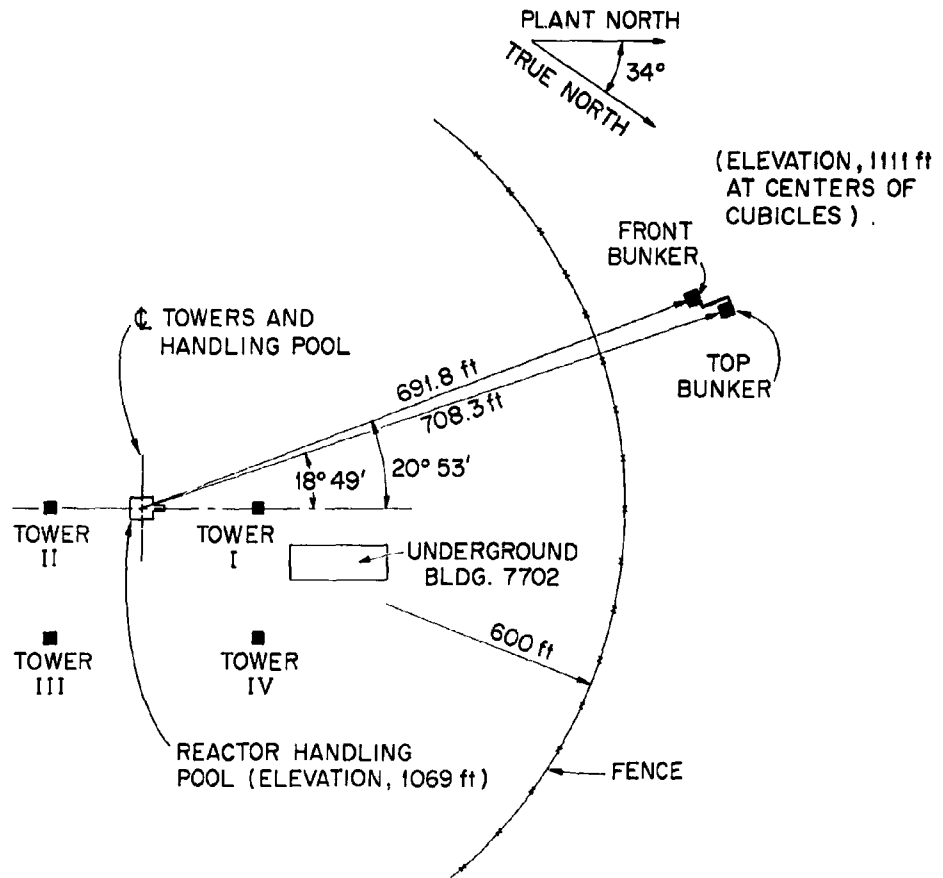


Fig. 2. Location of Concrete Bunkers and Tunnels.

is contained in the lower section of a cylindrical tank with a hemispherical bottom. The presence of water and auxiliary lead shielding above the top of the core prevents the uniform emission of radiation in about 50% of the  $2\pi$  solid angle in the upper hemisphere; however, the remaining 50% plus the uniform radiation emitted by the lower hemisphere simulates an isotropic source, such as a weapon burst, fairly well.

During this experiment the spectra of radiations emitted by the TSR-II were modified by the addition of a lead-water shield to the outside of the cylindrical tank. A general description of this shield, identified as COOL-I and shown in the left half of Fig. 3, may be found elsewhere.<sup>2</sup> The neutron-leakage spectrum for this shield is shown in Fig. 4. (The spectrum shown in the lower part of Fig. 4 is for the COOL-II shield shown in the right half of Fig. 3, but COOL-II was not used in this experiment.)

#### BUNKER DESCRIPTION

The two concrete-lined bunkers, which were 12-ft cubicles, were constructed so that the shields on the front face of one and on the top face of the other could be varied as shown in Fig. 5. The thickness of concrete and dirt surrounding all other faces was sufficient to make them black to the incident radiation. The bunkers were connected by a three-legged passageway or tunnel, 3 ft wide and 8 ft high, the two legs opening into the bunkers being perpendicular to and at opposite ends of the middle leg. The distance along the first leg of the passageway from the bunker with the variable front face, called the "front" bunker, to the center line of the middle leg was 6 ft 4 in. Similarly, the length along the third leg from the bunker with the variable top face, called the "top" bunker, to the center line of the middle leg was 6 ft 4 in., the entire length of the middle leg being 15 ft 2 in. The lower end of a 3-ft-diam, 7-ft 7-in.-high entranceway, covered by a 1-ft-thick concrete hatch, opened into the center of the ceiling of the middle leg.

2. F. J. Muckenthafer, L. B. Holland, and R. E. Maerker, In-Air Radiation Measurements in the Vicinity of the Tower Shielding Reactor II, ORNL-2337 (1963).

UNCLASSIFIED  
ORNL-LR-DWG 67012R

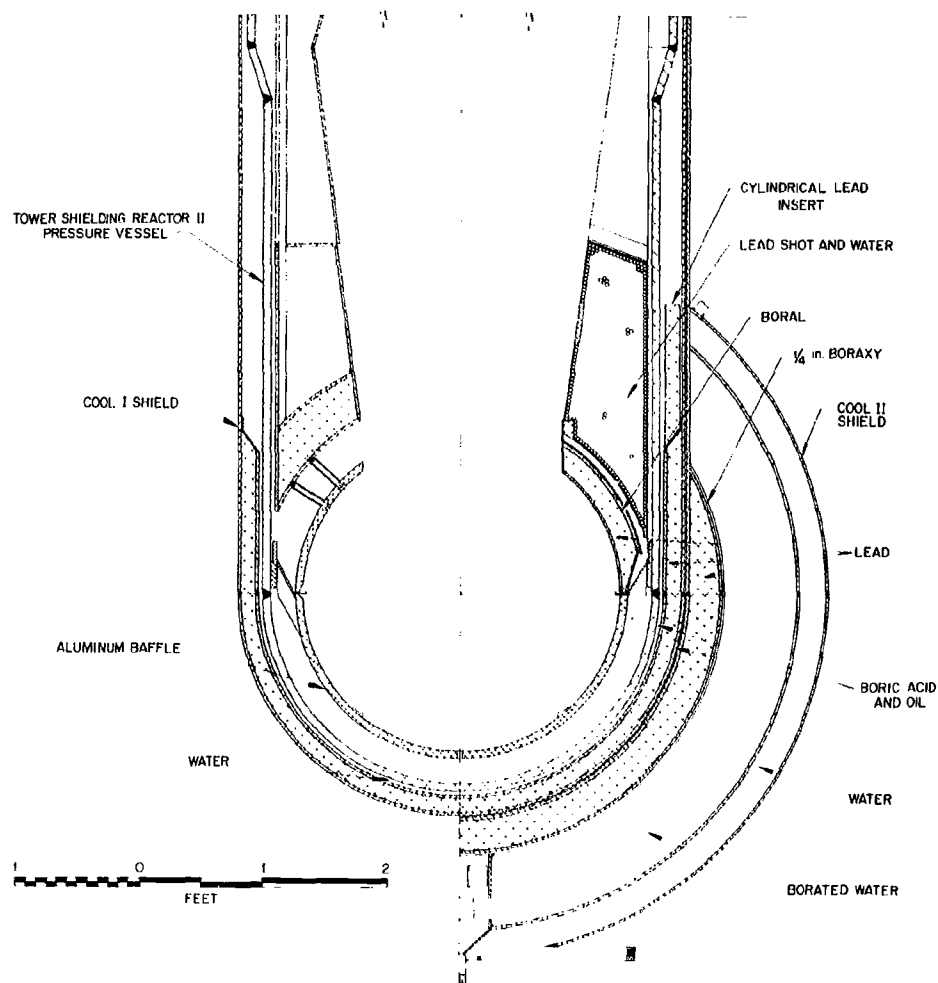


Fig. 3. TSR-II Shields COOL-I and COOL-II.

UNCLASSIFIED  
2-01-056-32-1416R1

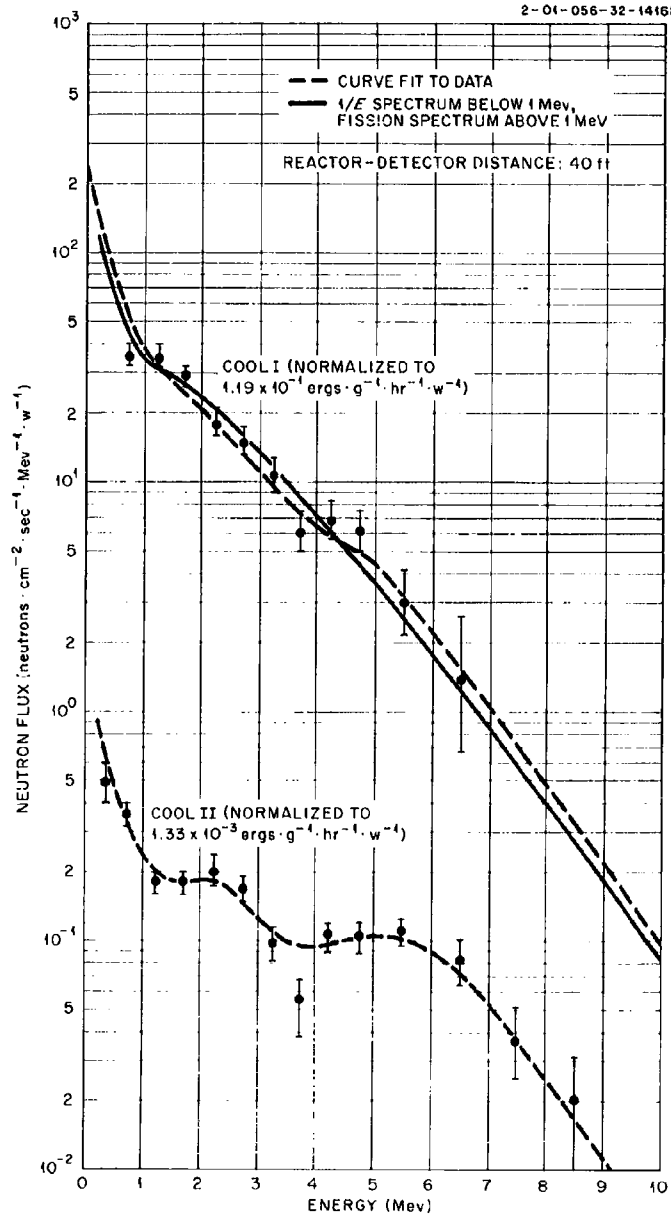


Fig. 4. Neutron-Leakage Spectra of TSR-II Shields.

UNCLASSIFIED  
2-DI-056-059-1406R1

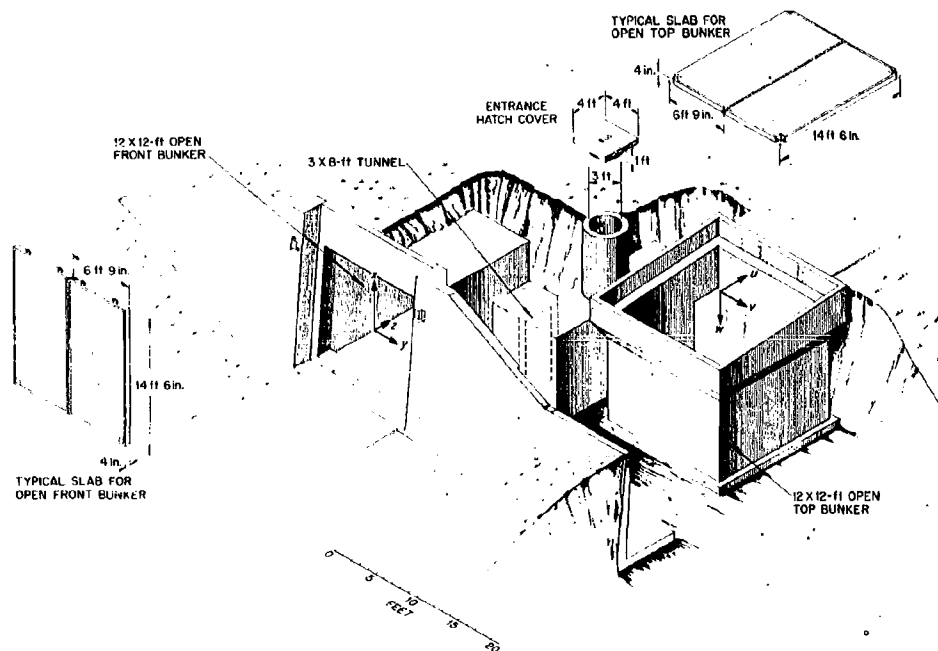


Fig. 5. Schematic of Bunker-Tunnel Arrangement, Showing the Coordinate Systems.

Five concrete shields were available for the open face of each bunker, varying in thickness from 4 to 20 in. in 4-in. steps. Because of their large size, the shields were made in two sections and required 1/2-in. steel reinforcing bars on 4-in. centers running the long dimension and 3/8-in. bars on 6-in. centers running the short dimension. The composition of a concrete sample taken from one of the slabs was analyzed to contain the following:

<u>Element</u>	<u>Weight Percent</u>
Aluminum	2.65
Calcium	22.12
Carbon	4.83
Hydrogen	0.36
Iron	1.32
Magnesium	0.85
Oxygen	47.04
Silicon	20.83

The coordinate systems used for most of the measurements in the experiment are shown in Fig. 5. Note that in each case the origin is the center of the inside face of the variable shield.

#### INSTRUMENT DESCRIPTION

The instruments used in the experiment consisted of an anthracene scintillation crystal, a Hurst-type proportional counter, a  $\text{BF}_3$  proportional counter, and a 3 x 3 in. NaI crystal.

The anthracene crystal, which was used for gamma-ray dose-rate measurements, was mounted on a photomultiplier tube whose current was read with a d-c integrator. Since the pulse output of the integrator was proportional to the current input, the automatic plotting equipment that requires a pulse signal could be used. The counter was calibrated against the known intensity from a  $\text{Co}^{60}$  source.

The appreciable response that the anthracene crystal has to neutron interactions within the crystal has not been corrected for in the data presented here. The portion of the response due to fast-neutron interactions can be estimated from data taken by General Dynamics/Fort Worth<sup>3</sup>

3. K. R. Spearman, Jr., Neutron Sensitivity of Anthracene Dosimeters, NARF-55-67T (Oct. 1955).

with similar counters. If it is assumed that the fast neutrons have a fission energy spectra, the GD/FW data yield an equivalent gamma-ray response of  $0.125 \text{ erg/g}_{\text{tissue}}$  per  $\text{erg/g}_{\text{tissue}}$  of fast-neutron dose. The anthracene crystal also has a significant response to thermal-neutron fields. This effect was cursorily investigated by making measurements (see Fig. 6), with and without a stainless-steel-canned  $\text{Li}^6$  shield surrounding the dosimeter, along the center line of the second and third legs of the tunnel leading from the front bunker (with no front shield) to the top bunker (with a full 20-in. top shield). An estimate of the thermal-neutron-induced response was obtained by using the ratio of the difference between the bare- and  $\text{Li}^6$ -covered-counter data to the thermal-neutron-flux data at the same location. The region from  $D = 0$  to 3 ft was ignored because of the complications introduced by the high fast-neutron dose present. The region from  $D = 3$  to 7 ft gave an estimate of  $3.6 \times 10^{-5} \text{ erg.g}_{\text{tissue}}^{-1} \cdot \text{hr}^{-1}$  equivalent gamma-ray response per unit thermal-neutron flux. The data from  $L = 1$  to 14 ft, in a region where the neutrons are quite thermal (the cadmium ratio, or ratio of bare  $\text{BF}_3$  to cadmium-covered  $\text{BF}_3$  readings, is around 70), gave an estimate of  $6.3 \times 10^{-5} \text{ erg.g}_{\text{tissue}}^{-1} \cdot \text{hr}^{-1}$  equivalent gamma-ray response per unit thermal-neutron flux.

The calibration procedure for the Hurst-type proportional counter, which was used for fast-neutron dose-rate measurements, involved first setting the system gain with a known gamma-ray dose rate and then reading the counter in a known field from a fast-neutron source. In particular, the system gain was set so that a  $\text{Co}^{60}$  gamma-ray dose rate of 2 r/hr produced 40 pulses per minute larger than 6 v at the output of the linear amplifier. The pulse output from the amplifier was integrated for the neutron dose readings so as to obtain an output proportional to the ionization in the chamber for neutrons. A Po-Be source was used for the daily calibrations of the counter.

The  $\text{BF}_3$ -filled proportional counter was used for thermal-neutron flux measurements. Although the output from the counter more closely resembles neutron density than neutron flux, because of the nearly  $1/v$  behavior of the  $\text{B}^{10}(n, \alpha)$  cross section, the readings were normalized to cadmium-difference measurements taken with gold foils in the radiation field from



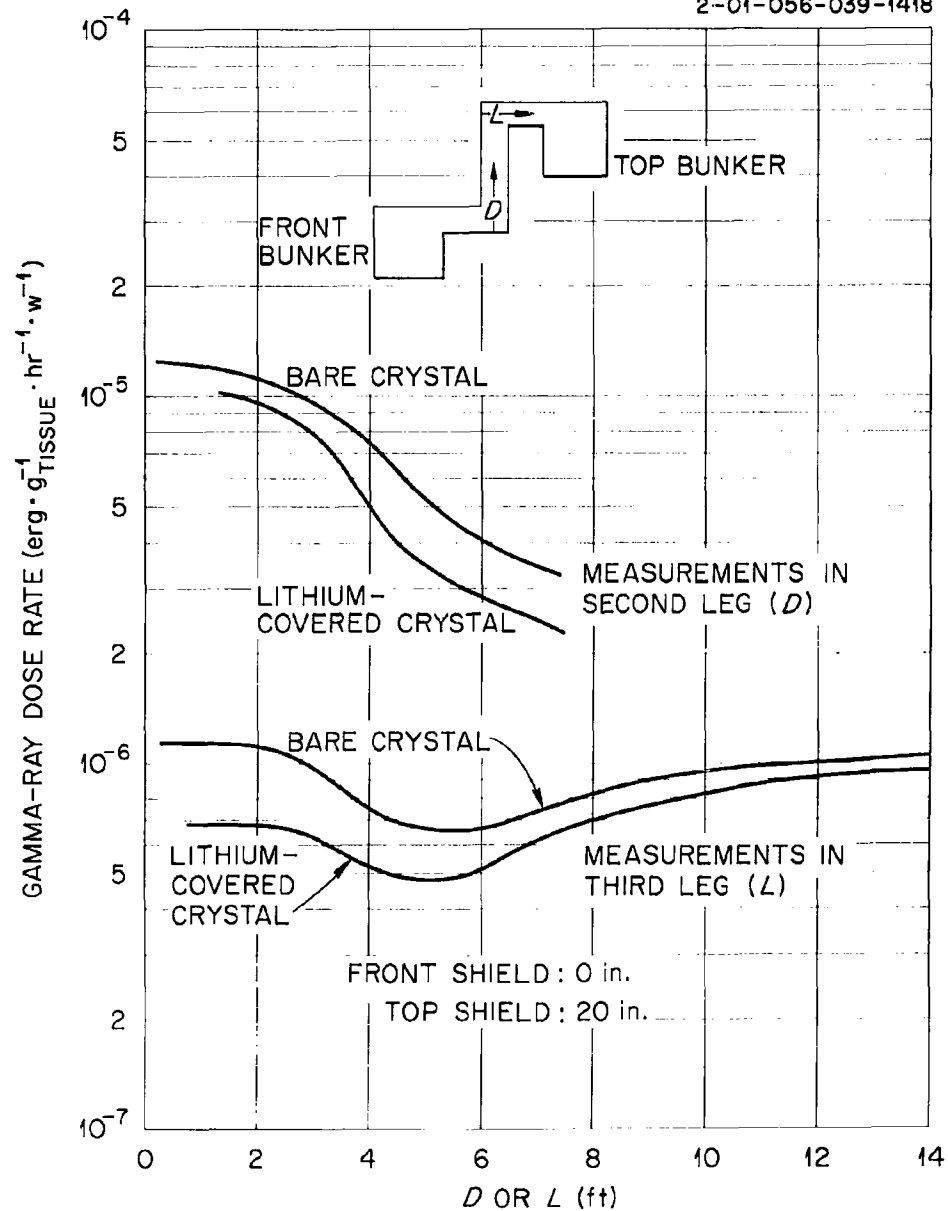
UNCLASSIFIED  
2-01-056-039-1418

Fig. 6. Investigation of Effect of Thermal-Neutron Response of Anthracene Crystal: Gamma-Ray Dose Rates in Second and Third Legs of Tunnel With and Without Li<sup>6</sup> Shield Surrounding Crystal.

the reactor. The daily calibrations were checked with a Po-Be source in a Lucite moderator.

The NaI crystal, which was used to determine gamma-ray pulse-height spectra, was mounted on a 3-in. photomultiplier tube. The pulse output from this counter was recorded with a 256-channel pulse-height analyzer. Energy calibrations were made against  $\text{Cs}^{137}$  and  $\text{Co}^{60}$  sources and the  $\text{C}^{12}$  decay gamma rays from a Po-Be source.

#### DOSE-RATE AND FLUX MEASUREMENTS IN BUNKERS

The first series of dose-rate and flux measurements in the bunkers were for fixed counter positions and various reactor altitudes in order to determine the effect of reactor height on the experimental results. The measurements, plotted in Figs. 7 and 8 for fast neutrons and gamma rays, respectively, were made in the front bunker (lower curves) fully shielded with 20 in. of concrete and in the top bunker (upper curves) shielded with 4 in. of concrete. It was concluded from these data that it would not be worthwhile, at least for this experiment, to take measurements at more than one altitude. Consequently, the rest of the measurements were taken at a reactor altitude of 100 ft, for the various parameters shown in Table 1. At this altitude a line from the reactor center to the center of the shield on the front bunker was perpendicular to the shield, and the line from the reactor center to the center of the shield on the top bunker struck the shield at a grazing angle of  $9.5^\circ$ .

Also in these series of measurements the effect of shield placement on the open faces of the bunkers was investigated by recessing the 4-in.-thick top shield 16 in. below ground level and then keeping it flush with the ground level. As can be seen by comparing the two upper curves in Figs. 7 and 8, there was negligible difference between the results for the two slab positions. Therefore all later measurements were taken with the slab recessed, since this position was more convenient.

Most of the later measurements in the bunkers were made as a function of one of the variables defined in the rectangular coordinate systems shown in Fig. 5. Unless otherwise specified, all data taken in the top bunker were for the case of a full front shield on the front bunker, and vice versa (although this was found to be unnecessary, as will be seen below).

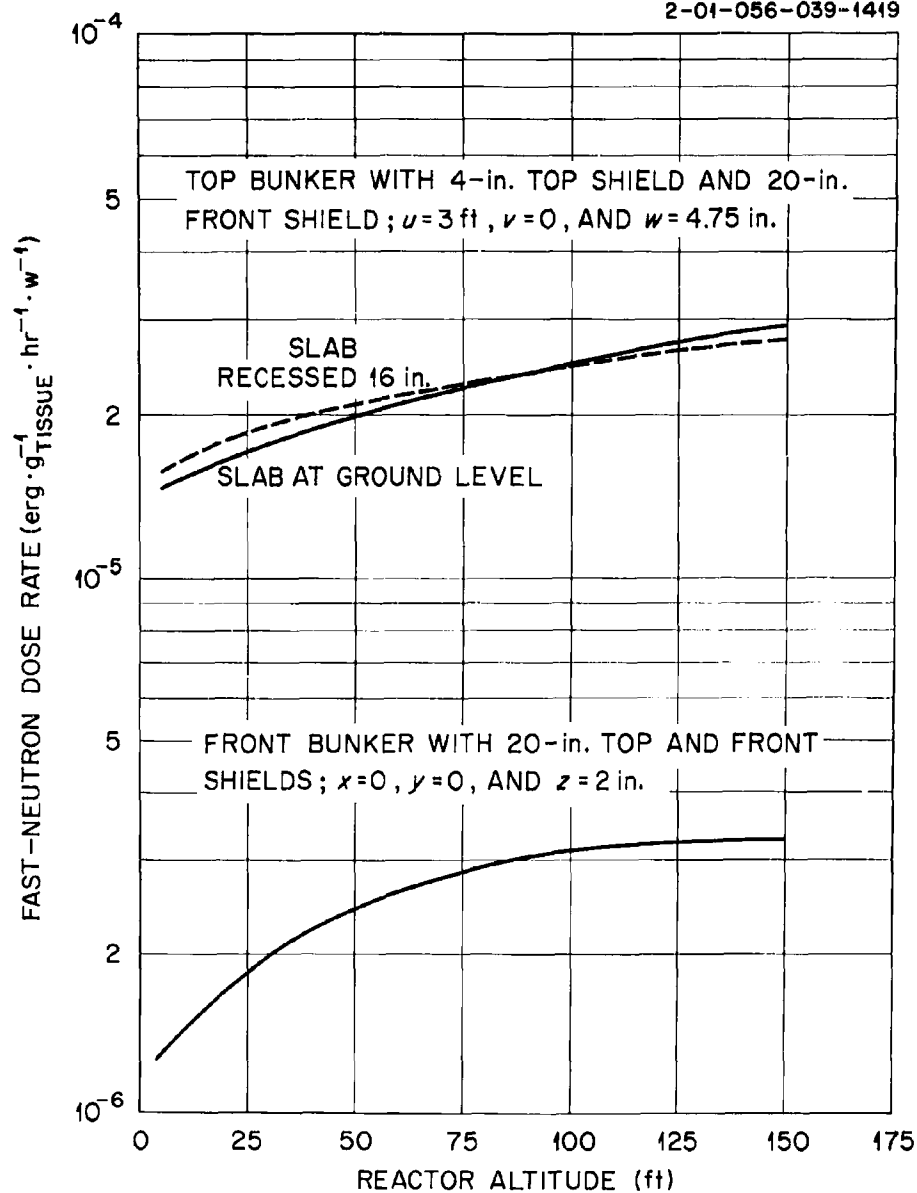
UNCLASSIFIED  
2-01-056-039-1419

Fig. 7. Fast-Neutron Dose Rates in Front and Top Bunkers as a Function of Reactor Altitude.

UNCLASSIFIED  
2-01-056-039-1420

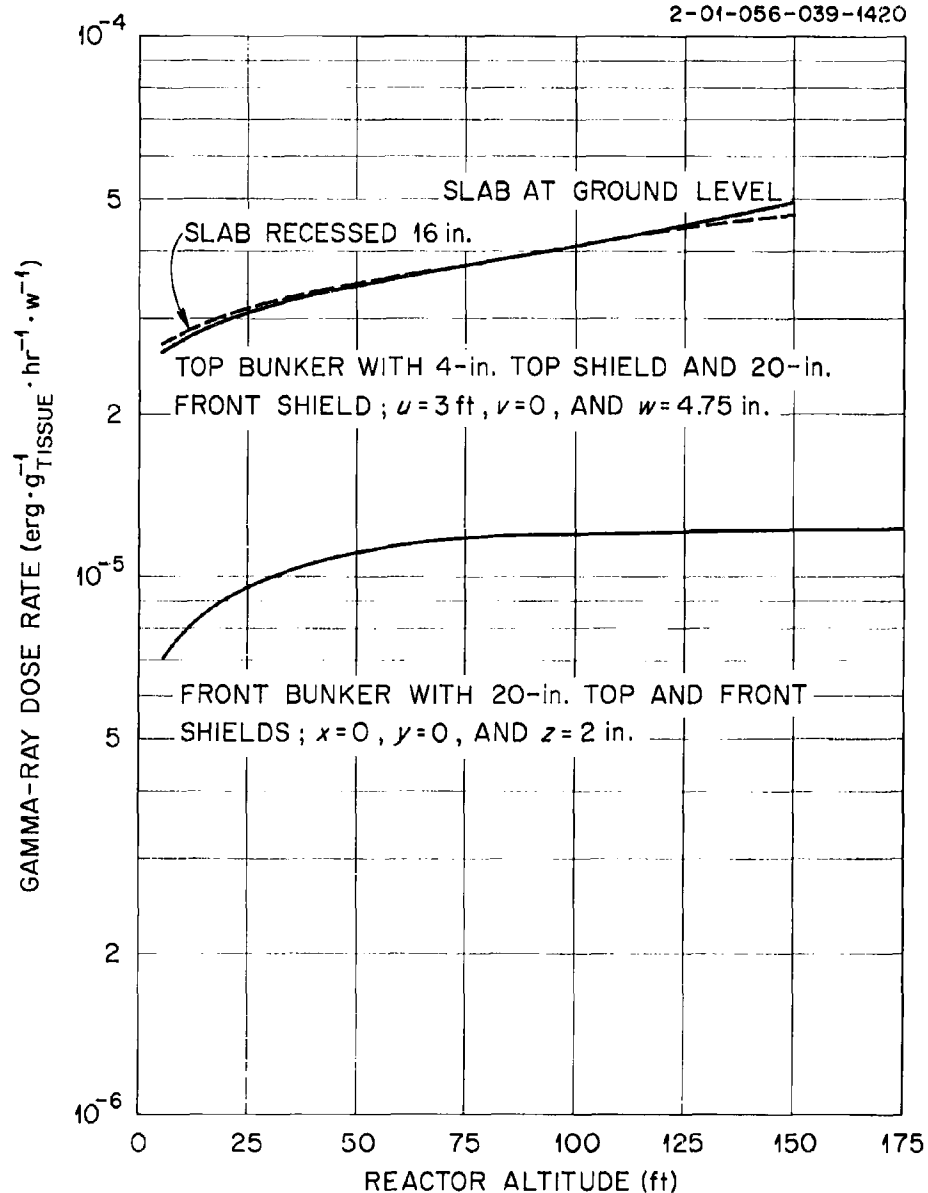


Fig. 8. Gamma-Ray Dose Rates in Front and Top Bunkers as a Function of Reactor Altitude.

Table 1. Summary of Experimental Parameters

Location of Measurement	Shield Thickness (in.)		Type of Measurement	Coordinates			Figure Number
	Top Bunker	Front Bunker		x, u	y, v	z, w	
Front bunker	20	0	Fast-neutron dose rate	0	0	Variable	9
	20	4					
	20	8					
	20	12					
	20	16					
	20	20					
Front bunker	20	0	Gamma-ray dose rate	0	0	Variable	10
	20	4					
	20	8					
	20	12					
	20	16					
	20	20					
Front bunker	20	0	Thermal-neutron flux	0	0	Variable	11
	20	4					
	20	8					
	20	12					
	20	16					
	20	20					
Front bunker	20	20	Gamma-ray dose rate	0	0	Variable	12
	20	20					
Top bunker	0	20	Fast-neutron dose rate	- 3'	5.54'	Variable	12
	4	20					
	8	20					
	12	20					
	16	20					
	20	20					
Top bunker	0	20	Fast-neutron dose rate	- 2.5'	5.54'	Variable	12
	4	20					
	8	20					
	12	20					
	16	20					
	20	20					
Top bunker	0	20	Fast-neutron dose rate	0	0	Variable	13
	4	20					
	8	20					
	12	20					
	16	20					
	20	20					

Table 1 (cont.)

Location of Measurement	Shield Thickness (in.)		Type of Measurement	Coordinates			Figure Number
	Top Bunker	Front Bunker		x, u	y, v	z, w	
Top bunker	0	20	Gamma-ray dose rate	0	0	Variable	14
	4	20					
	8	20					
	12	20					
	16	20					
	20	20					
Top bunker	0	20	Thermal-neutron flux	0	0	Variable	15
	4	20					
	8	20					
	12	20					
	16	20					
	20	20					
Top bunker	0	20	Fast-neutron dose rate	Variable	0	6'	16
	4	20					
	12	20					
Top bunker	0	20	Gamma-ray dose rate	Variable	0	6'	17
	4	20					
	12	20					
	20	20					
Top bunker	0	20	Thermal-neutron flux	Variable	0	6'	18
	4	20					
	12	20					
	20	20					
Top bunker	0	20	Fast-neutron dose rate	Variable	0	4.75"	19
	4	20					
	12	20					

Table 1 (cont.)

Location of Measurement	Shield Thickness (in.)		Type of Measurement	Coordinates			Figure Number
	Top Bunker	Front Bunker		x, u	y, v	z, w	
Top bunker	0	20	Gamma-ray dose rate	Variable	0	4.75"	20
	4	20					
	12	20					
	20	20					
Top bunker	0	20	Fast-neutron dose rate	Variable	5'9"	6'	21
	4	20					
	12	20					
	20	20					
Top bunker	0	20	Gamma-ray dose rate	Variable	5'9"	6'	22
	4	20					
	12	20					
	20	20					
Top bunker	0	20	Thermal-neutron flux	Variable	5'9"	6'	23
	4	20					
	12	20					
	20	20					
Top bunker	20	0	Gamma-ray dose rate	Variable	-5'1"	8'2"	24
	20	20		Variable	-5'1"	8'2"	24
	20	0	Fast-neutron dose rate	Variable	-5'1"	8'2"	24
Top bunker	0	20	Fast-neutron dose rate	Variable	0	4.75"	25
				Variable	0	6'	25
				Variable	5'9"	6'	25
Top bunker	0	20	Thermal-neutron flux	Variable	0	6'	26
				Variable	5'9"	6'	26
Top bunker	4	20	Fast-neutron dose rate	Variable	0	4.75"	27
				Variable	0	6'	27

Table 1 (cont.)

Location of Measurement	Shield Thickness (in.)		Type of Measurement	Coordinates			Figure Number
	Top Bunker	Front Bunker		x, u	y, v	z, w	
Top bunker	4	20	Gamma-ray dose rate	Variable	0	4.75"	28
				Variable	0	6'	28
Top bunker	12	20	Fast-neutron dose rate	Variable	0	4.75"	29
				Variable	5'7.5"	6.5"	29
				Variable	0	6'	29
				Variable	5'9"	6'	29
Top bunker	12	20	Gamma-ray dose rate	Variable	0	4.75"	30
				Variable	5'7.5"	12.5"	30
				Variable	0	6'	30
				Variable	5'9"	6'	30
Top bunker	20	20	Gamma-ray dose rate	Variable	0	4.75"	31
				Variable	5'7.5"	12.5"	31
				Variable	0	6'	31
				Variable	5'9"	6'	31
				Variable	0	11'7.5"	31
Top bunker	20	20	Thermal-neutron flux	Variable	0	4.5"	32
				Variable	0	6'	32
				Variable	5'9"	6'	32
				Variable	0	11'7.5"	32
Front bunker, with shadow shield	20	0, 4	Fast-neutron dose rate	0	Variable	6'	33
Front bunker, with shadow shield	2 in. polyethylene, 2 in. borated polyethylene, and 4 in. concrete <sup>a</sup>	0, 4	Gamma-ray dose rate	0	Variable	6'	34



Table 1 (cont.)

Location of Measurement	Shield Thickness (in.)		Type of Measurement	Coordinates			Figure Number
	Top Bunker	Front Bunker		x, u	y, v	z, w	
Front bunker, with shadow shield	2 in. polyethylene, 2 in. borated polyethylene, and 4 in. concrete <sup>a</sup>	0, 4	Thermal-neutron flux	0	Variable	6'	35
From rear of front bunker to 30 ft in front of bunker	20	0	Fast-neutron and gamma-ray dose rates and thermal-neutron flux	0	0	Variable	36
Tunnel, all three legs	20	0	Fast-neutron and gamma-ray dose rates and thermal-neutron flux	Measurement made along center line of tunnel			37
Tunnel, middle leg <sup>c</sup>	20	0	Fast-neutron dose rate	Measurement made along center line of tunnel			38
	20	4	Fast-neutron dose rate				38
	20	12	Fast-neutron dose rate				38
	20	20	Fast-neutron dose rate				38
	20	4(W); 0(E) <sup>b</sup>	Fast-neutron dose rate				38
	20	0(W); 4(E) <sup>b</sup>	Fast-neutron dose rate				38
	20	12(W); 0(E) <sup>b</sup>	Fast-neutron dose rate				38
	20	0(W); 12(E) <sup>b</sup>	Fast-neutron dose rate				38

Table 1 (cont.)

Location of Measurement	Shield Thickness (in.)		Type of Measurement	Coordinates			Figure Number
	Top Bunker	Front Bunker		X, U	Y, V	Z, W	
Tunnel, middle legs <sup>c</sup>	20	0	Gamma-ray dose rate	Measurements made along center line of tunnel			39
	20	4	Gamma-ray dose rate				39
	20	12	Gamma-ray dose rate				39
	20	20	Gamma-ray dose rate				39
	20	0(E); 4(W) <sup>b</sup>	Gamma-ray dose rate				39
	20	4(E); 0(W) <sup>b</sup>	Gamma-ray dose rate				39
	20	0(E); 12(W) <sup>b</sup>	Gamma-ray dose rate				39
	20	12(E); 0(W) <sup>b</sup>	Gamma-ray dose rate				39
Tunnel, all three legs	0	20	Fast-neutron and gamma-ray doses and thermal-neutron flux	Measurement made along center line of tunnel			40
In center of top bunker	0 4 20	0	Gamma-ray pulse-height spectra	0	0	6'	41
In center of top bunker	4	0	Gamma-ray pulse-height spectra	0	0	6'	42
	2 in. borated polyethylene and 4 in. concrete <sup>a</sup>	0	Gamma-ray pulse-height spectra				
	2 in. polyethylene, 2 in. borated polyethylene, and 4 in. concrete <sup>a</sup>	0	Gamma-ray pulse-height spectra	0	0	6'	42

Table 1 (cont.)

Location of Measurement	Shield Thickness (in.)		Type of Measurement	Coordinates			Figure Number
	Top Bunker	Front Bunker		x, u	y, v	z, w	
In center of middle leg of tunnel	20	0	Gamma-ray pulse-height spectra	Measurement made in center of tunnel			43

a. Listed in order from top layer down.

b. The numbers preceding (W) and (E) indicate the thickness of shield, in inches, on the west (left) side and east (right) side, respectively.

c. Includes measurement made while cover was removed from entrance hatch.

d. Measurements made with and without boron cover surrounding crystal.

Figures 9, 10, and 11\* show measurements of fast-neutron and gamma-ray dose rates and thermal-neutron fluxes, respectively, along the z axis of the front bunker for various front-shield thicknesses. The fast-neutron and gamma-ray dose rates shown in Fig. 12 were also obtained as a function of z, but for different x and y coordinates. For these latter measurements the full 20-in. shield was maintained on the front face.

Figures 13 through 24 all show the data obtained in the top bunker as a function of position within the bunker for several different top-shield thicknesses. Figure 23 is representative of measurements taken close to and across the opening to the interconnecting tunnel in order to determine whether variations in the shield on the front bunker affected measurements in the top bunker. The front-slab thickness was varied from 0 to 20 in. with less than a 10% effect observed in the gamma-ray dose rates and with virtually no effect observed in the fast-neutron dose rates.

Figures 25 through 32 consist primarily of cross plots of the data given in Figs. 13 through 23, each set of cross plots corresponding to a specific top-shield thickness. These data demonstrate the variations of radiation intensities with position in the bunker for a fixed shield.

One of the objectives of the experiment was to determine the relative contributions from each of the six surfaces of a cubicle to the intensities of the various radiations at the center of the cubicle. This was attempted experimentally by using a shadow shield to block the detector's view of one or more surfaces of the cubicle. Since most of the interest was in fast-neutron dose rates, the shadow shields were designed specifically for neutron attenuation. They were built of 4 x 4 x 8 in. lithiated-paraffin blocks consisting of 40 wt % lithium carbonate (natural lithium) and 60 wt % paraffin. The blocks were stacked so as to approximate a truncated pyramid 20 in. high with a 22-in. square top and a 58-in. square bottom. The two ends of the shadow shield were parallel to the surface being shielded, the small end being nearest the detector.

---

\*These figures and all succeeding figures are assembled as a group following the last page of text.

Figure 33 gives the results of the measurements taken in the front bunker with a fast-neutron dosimeter while various shadow shields were in position and the front face was either open or covered with a 4-in. shield. Horizontal traverses were made so as to obtain a normalization value at a point far enough from the shadow shields for the reading not to be excessively perturbed by the presence of the shadow shields. Each set of curves was normalized to the average reading obtained at  $y = 5$  ft.

Figures 34 and 35 give the corresponding shadow-shield data for gamma-ray dose rates and thermal-neutron fluxes, respectively. These data are somewhat more difficult to interpret because the shadow shield was not black to gamma rays and perturbed the thermal-neutron fluxes excessively. Figure 34 also shows the results of removing 4 in. from the large end of the front shadow shield, namely, a 14% increase in gamma-ray dose rate. The fast-neutron dose rate did not vary with this configuration change. The approximate relative contributions of each wall, as derived from the fast-neutron dose-rate data by taking differences of the various measurements, are shown below for the two front-shield configurations.

Shield on Front Face (in.)	Contribution (%)		
	Front	Side	Rear
0	77	4	7
4	75	5	5

Figure 36 shows measurements of fast-neutron and gamma-ray dose rates and thermal-neutron fluxes taken along the  $z$  axis of the front bunker with no shield on the front face. It will be noted that these measurements extended out the bunker to over the concrete pad in front of the bunker. Included as notes on the figure are values, at four positions, of the cadmium ratio, defined as the ratio of the measurements made with the bare  $\text{BF}_3$  counter to those with a cadmium-covered counter.

## DOSE-RATE AND FLUX MEASUREMENTS IN TUNNEL

Figures 37 through 40 give results of traverses along the center line of the interconnecting tunnel for various slab configurations on the bunkers. The data in Figs. 37, 38, and 39 were taken with the full shielding on the top bunker. In Fig. 37, which is for the case of no shield on the front bunker, the measurements are plotted as a function of the distance along the center line of the tunnel, starting from the x,z plane of the front bunker and continuing along the center lines of all three legs, as shown in the insert on the figure.

Figures 38 and 39 show the effects of various front-slab thicknesses on the fast-neutron and gamma-ray dose rates, respectively, measured along the center line of the long center leg of the tunnel. These data are plotted as a function of the distance from the tunnel wall closest to the source and include measurements for front-shield thicknesses of 0, 4, 12, and 20 in. The zero-thickness curves in these figures correspond to the data between 12.5 and 18.5 ft in Fig. 36.

Figures 38 and 39 also show measurements made with only one side of a front slab in place. The curve labels indicate the shield thickness on each side; that is, "4 in. W - 0 in. E" indicates that the west side of the front face of the bunker had a 4-in.-thick shield, whereas the east, or right, side was unshielded. Figures 37 and 38 also include measurements taken with a 20-in. shield on both bunkers but with the hatch removed from the entranceway.

Figure 40 shows data for no shield on the top bunker and for 20 in. on the front bunker plotted as a function of the distance along the center line of the tunnel, starting with the w,u plane of the top bunker. Except for the regions close to the bunkers, the shapes of these curves are quite similar to those in Fig. 36, which gives comparable data for no shield on the front bunker.

The data obtained in the tunnels illustrate the importance to the gamma-ray dose rates of the thermal-neutron captures in the tunnel walls, as evidenced by the similarity of shape of the gamma-ray dose-rate and thermal-neutron-flux curves. In order to calculate the production of

capture gamma rays in the walls, it was necessary to know the thermal-neutron flux distribution in the tunnel. To aid such calculations in this and similar geometries, an attempt was made to measure the angular distribution of thermal neutrons leaving a small area of the tunnel wall. The measurements were made with a 3-in.-diam  $\text{BF}_3$  counter whose housing was wrapped over its entire length with cadmium sheeting that extended 9 in. beyond the end of the counter, thus forming a collimator. The collimator was used to "view" from several angles a spot on the tunnel wall located at about the middle of the center leg. At each angle, measurements were made with and without a cadmium cover over the opening in the collimator, in order to correct for the contribution from the neutrons above the cadmium-cutoff energy. The results showed that, for angles from 0 to 60 deg from the normal to the wall, the fluxes were constant to within experimental error. This indicates a cosine distribution of the current leaving the wall, since the wall area seen by the counter through the collimator varies approximately as the inverse of the cosine of the polar angle.

#### GAMMA-RAY SPECTRA DETERMINATIONS

In an attempt to assess the relative importances of various sources of gamma rays, the pulse-height spectra of gamma rays in the center of both the tunnel and the top bunker with various top-slab configurations were determined with a 3-in. NaI crystal. Figure 41 shows pulse-height spectra obtained in the top bunker with top-shield thicknesses of 0, 4, and 20 in. Figure 42 repeats the 4-in.-slab data and also includes data for a top-slab configuration consisting of 2 in. of borated polyethylene and 4 in. of concrete and for one consisting of layers (from the top down) of 2 in. of polyethylene, 2 in. of borated polyethylene, and 4 in. of concrete. Figure 43 gives the data obtained in the tunnel, with and without a boron cover surrounding the crystal. Reduction of these data to incident spectra has not been accomplished at this time.

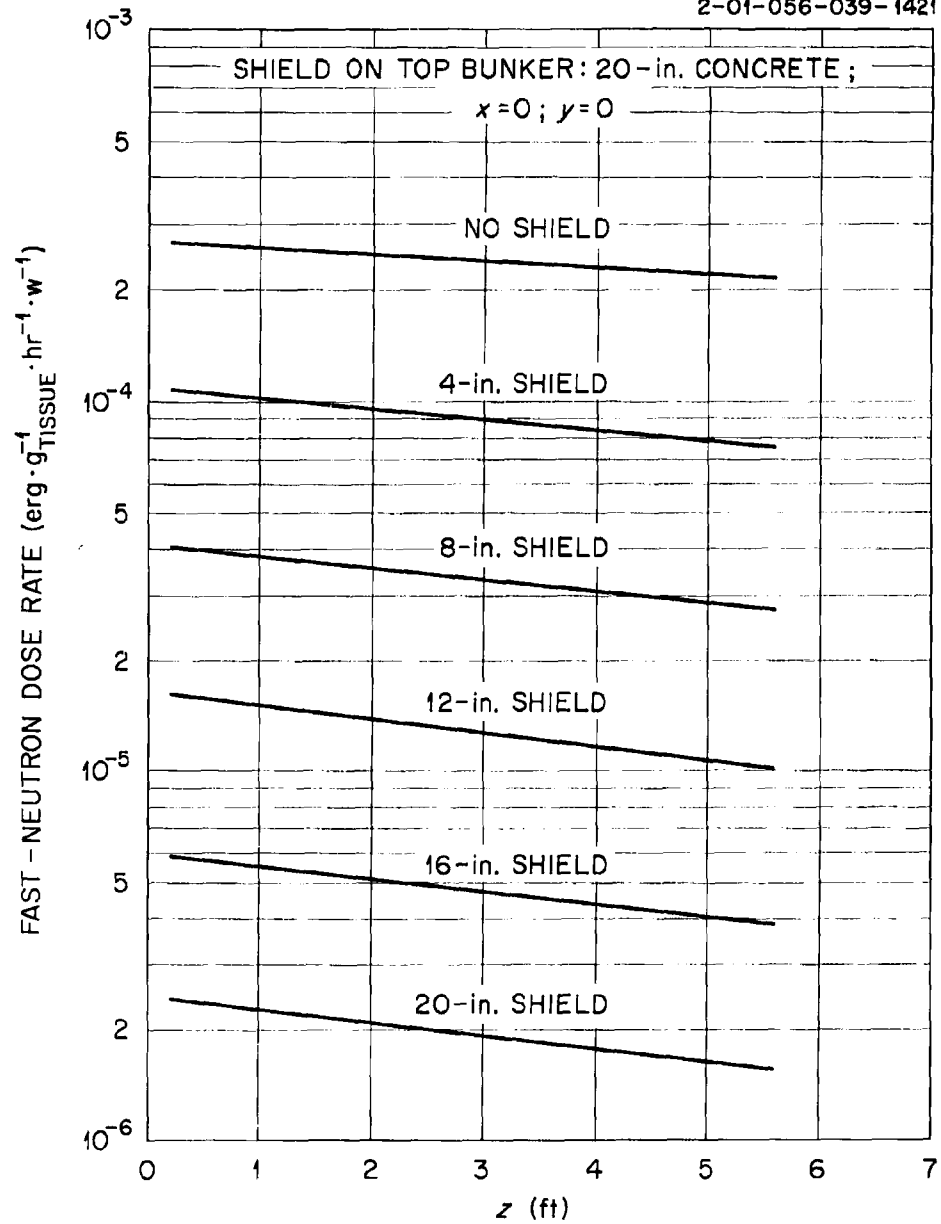
UNCLASSIFIED  
2-01-056-039-1421

Fig. 9. Fast-Neutron Dose Rates Along z Axis of Front Bunker for Various Shield Thicknesses on the Front Face.



UNCLASSIFIED  
2-01-056-039-1409

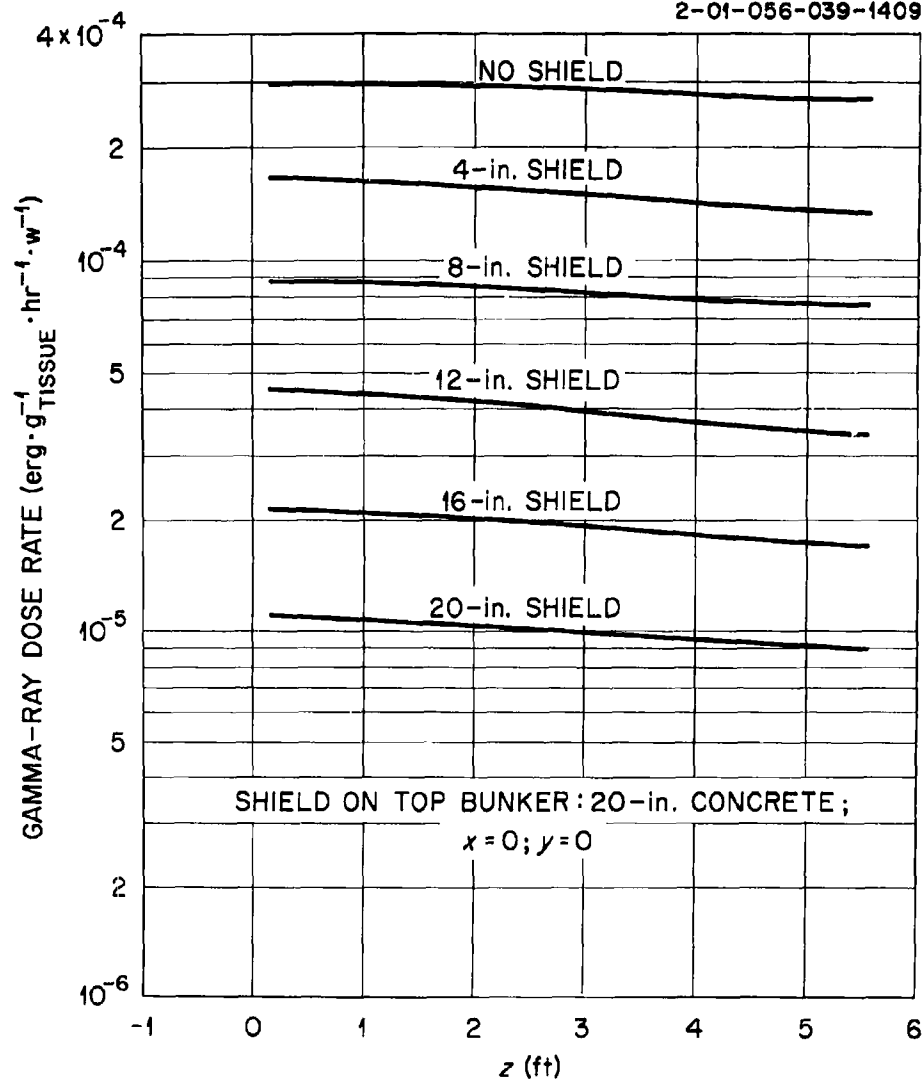


Fig. 10. Gamma-Ray Dose Rates Along  $z$  Axis of Front Bunker for Various Shield Thicknesses on the Front Face.

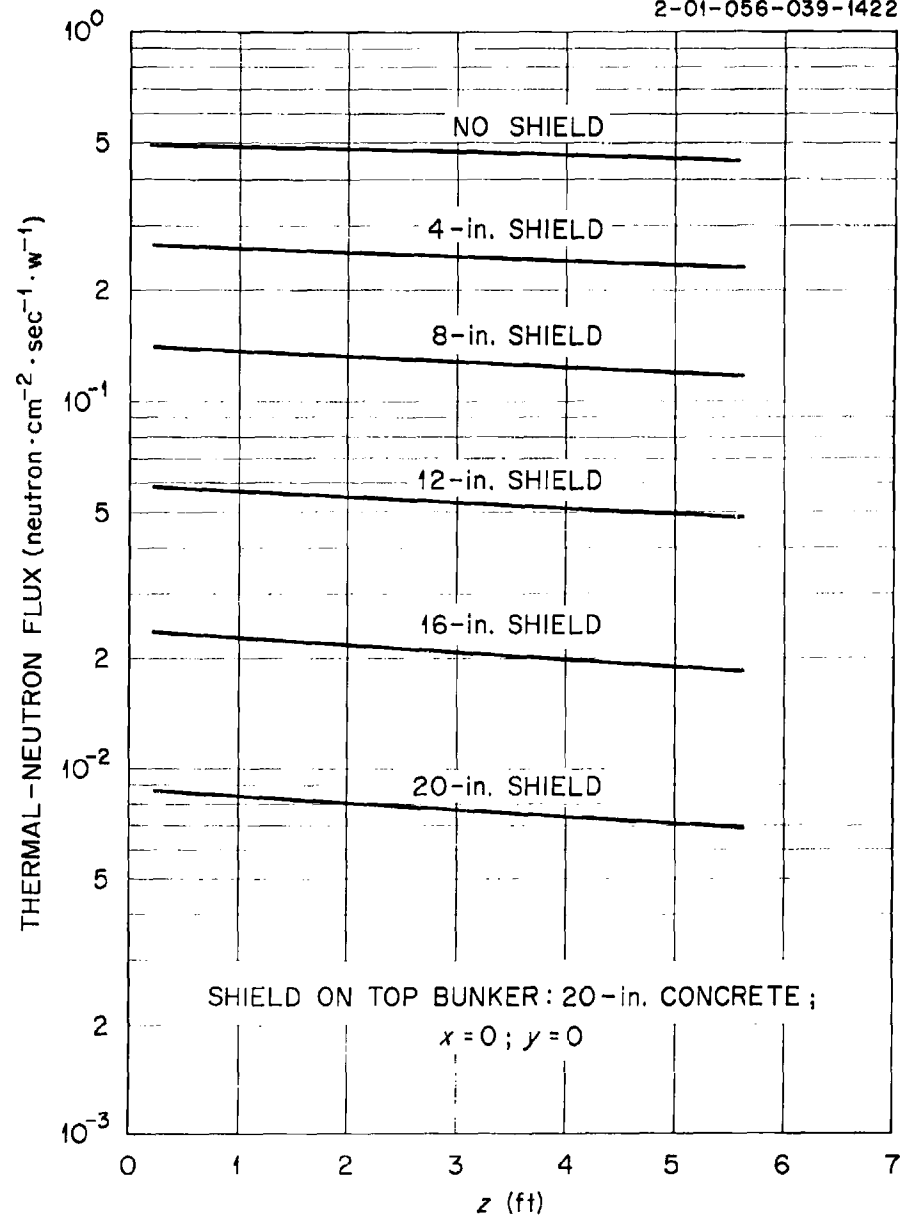
UNCLASSIFIED  
2-01-056-039-1422

Fig. 11. Thermal-Neutron Fluxes Along z Axis of Front Bunker for Various Shield Thicknesses on the Front Face.

UNCLASSIFIED  
2-01-056-039-1423

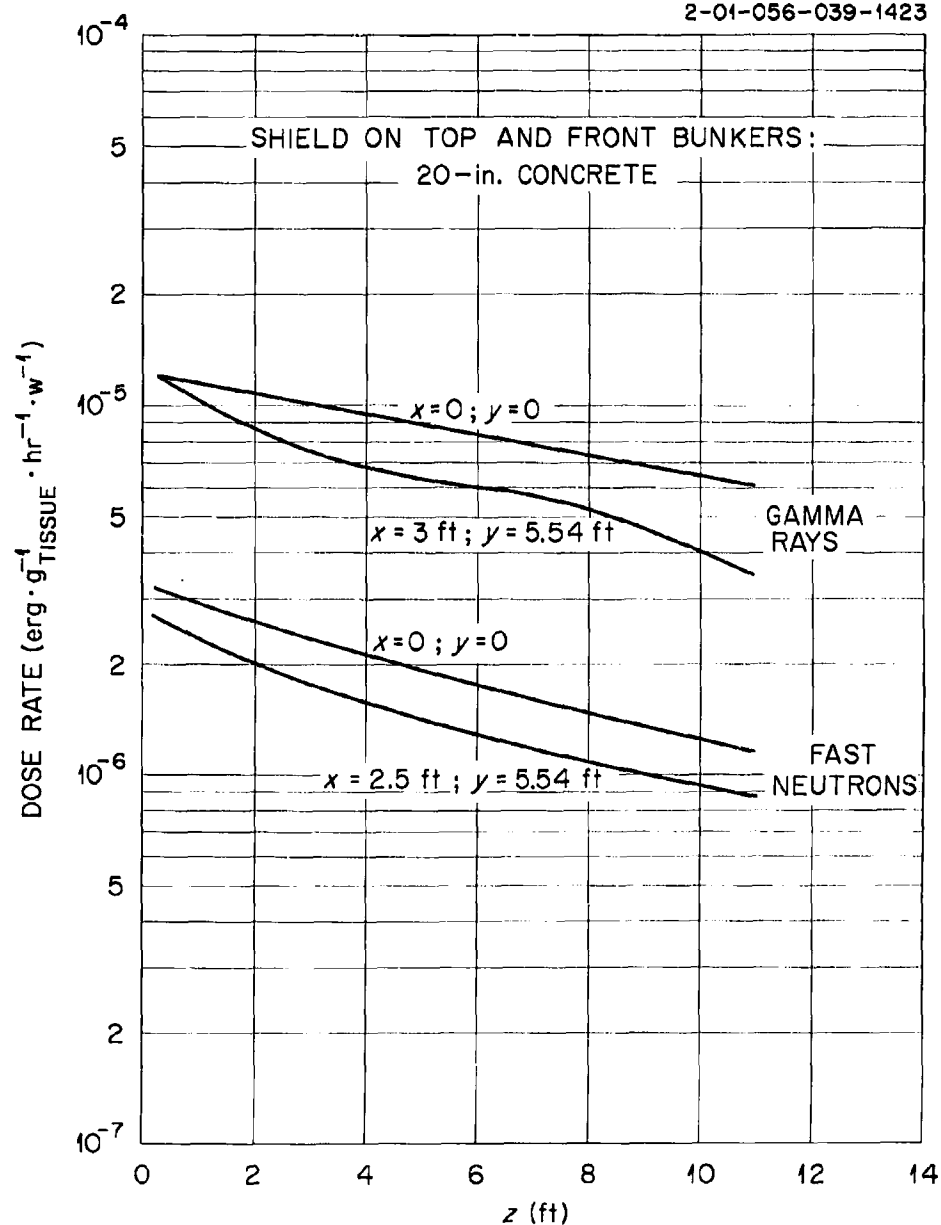


Fig. 12. Fast-Neutron and Gamma-Ray Dose Rates in Front Bunker as a Function of  $z$  Position for Various  $x$  and  $y$  Values.

UNCLASSIFIED  
2-01-056-039-1424

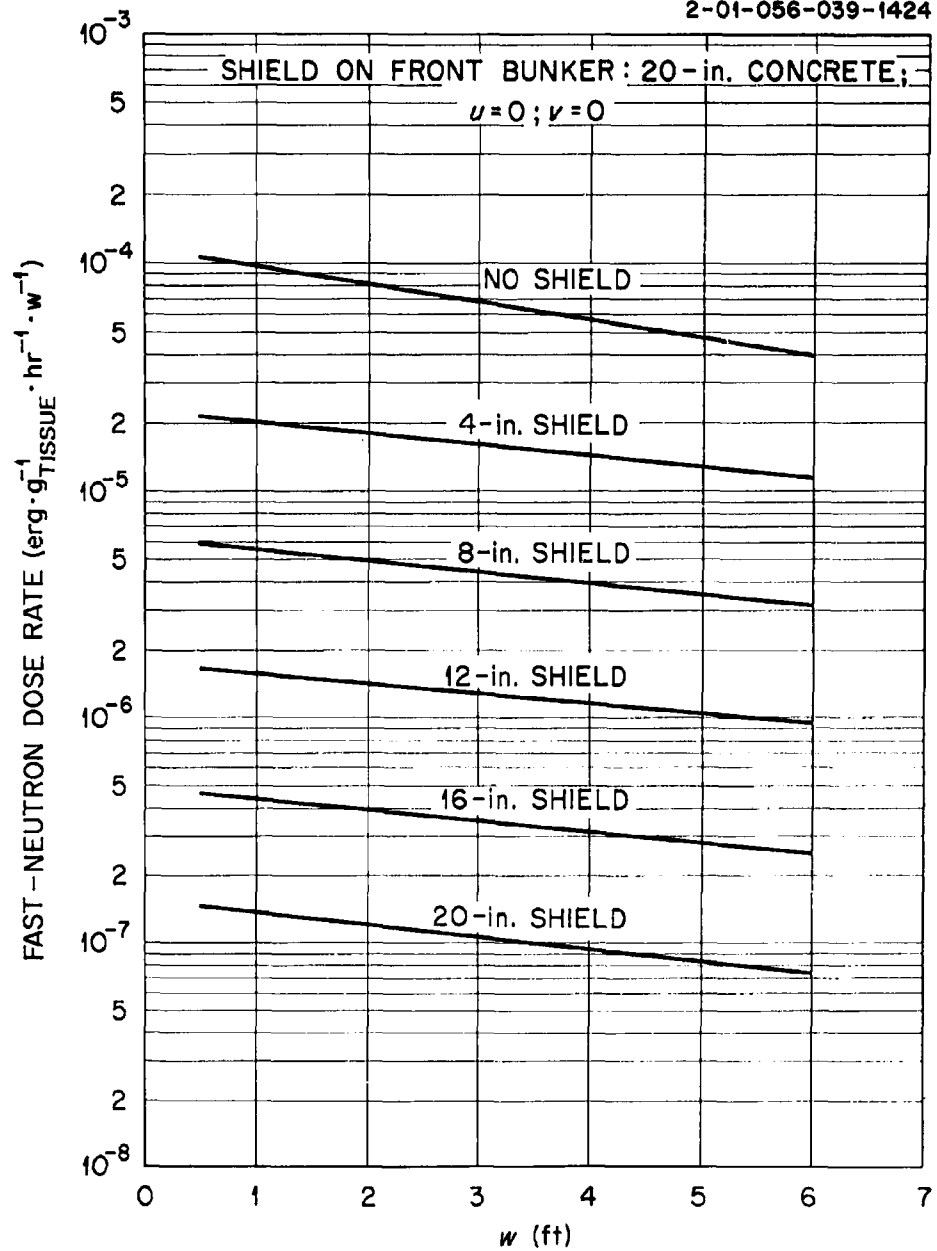


Fig. 13. Fast-Neutron Dose Rates Along  $w$  Axis of Top Bunker for Various Shield Thicknesses on the Top Face.

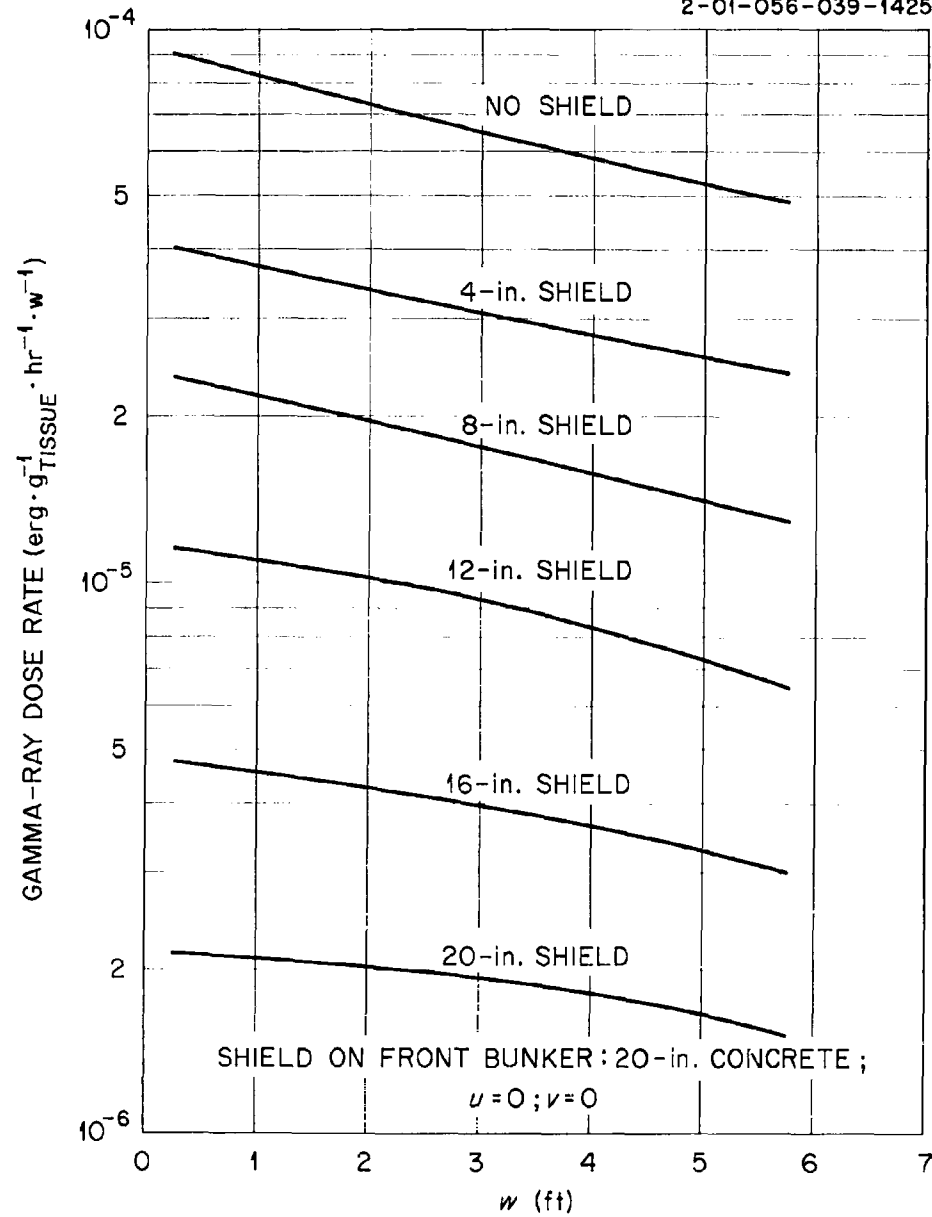
UNCLASSIFIED  
2-01-056-039-1425

Fig. 14. Gamma-Ray Dose Rates Along  $w$  Axis of Top Bunker for Various Shield Thicknesses on the Top Face.

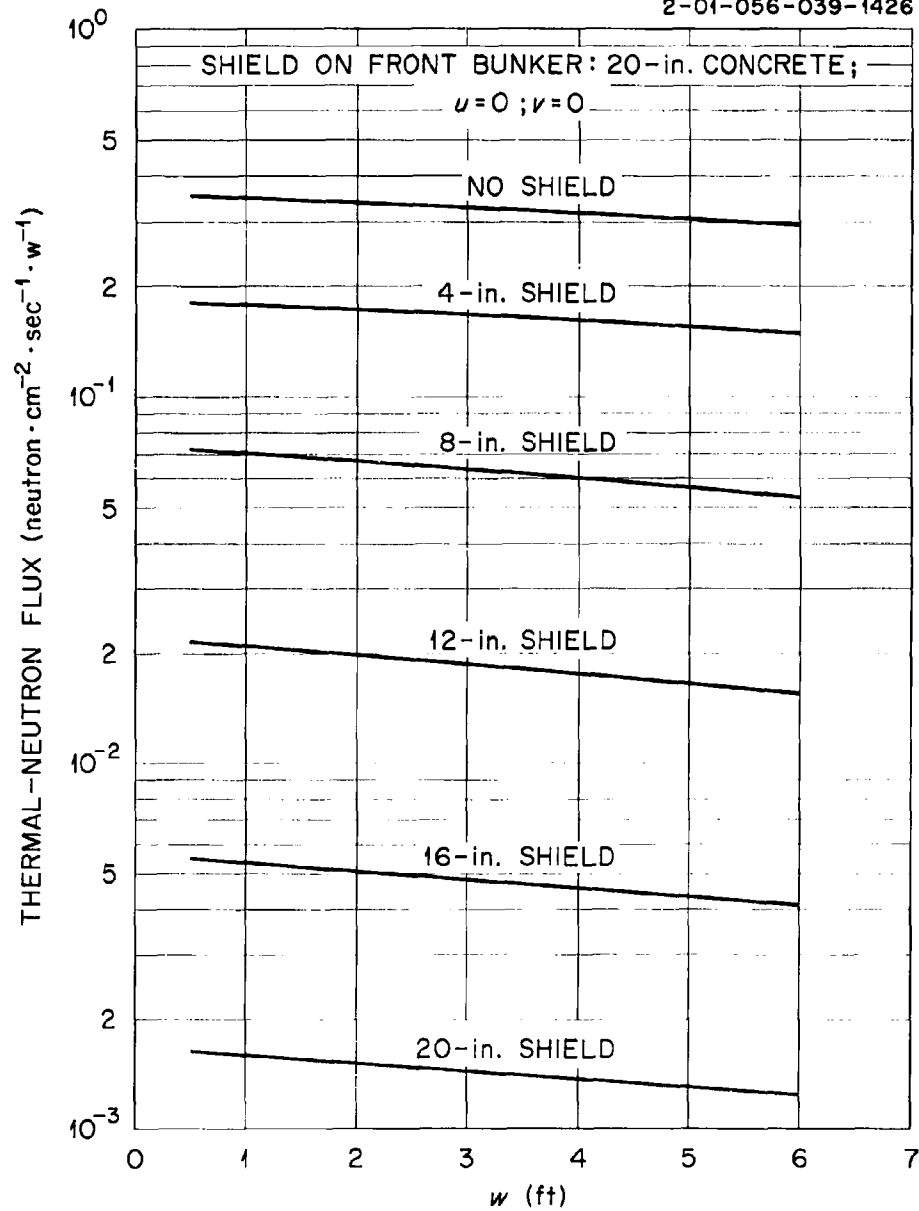


Fig. 15. Thermal-Neutron Fluxes Along w Axis of Top Bunker for Various Shield Thicknesses on the Top Face.

UNCLASSIFIED  
2-01-056-039-1427

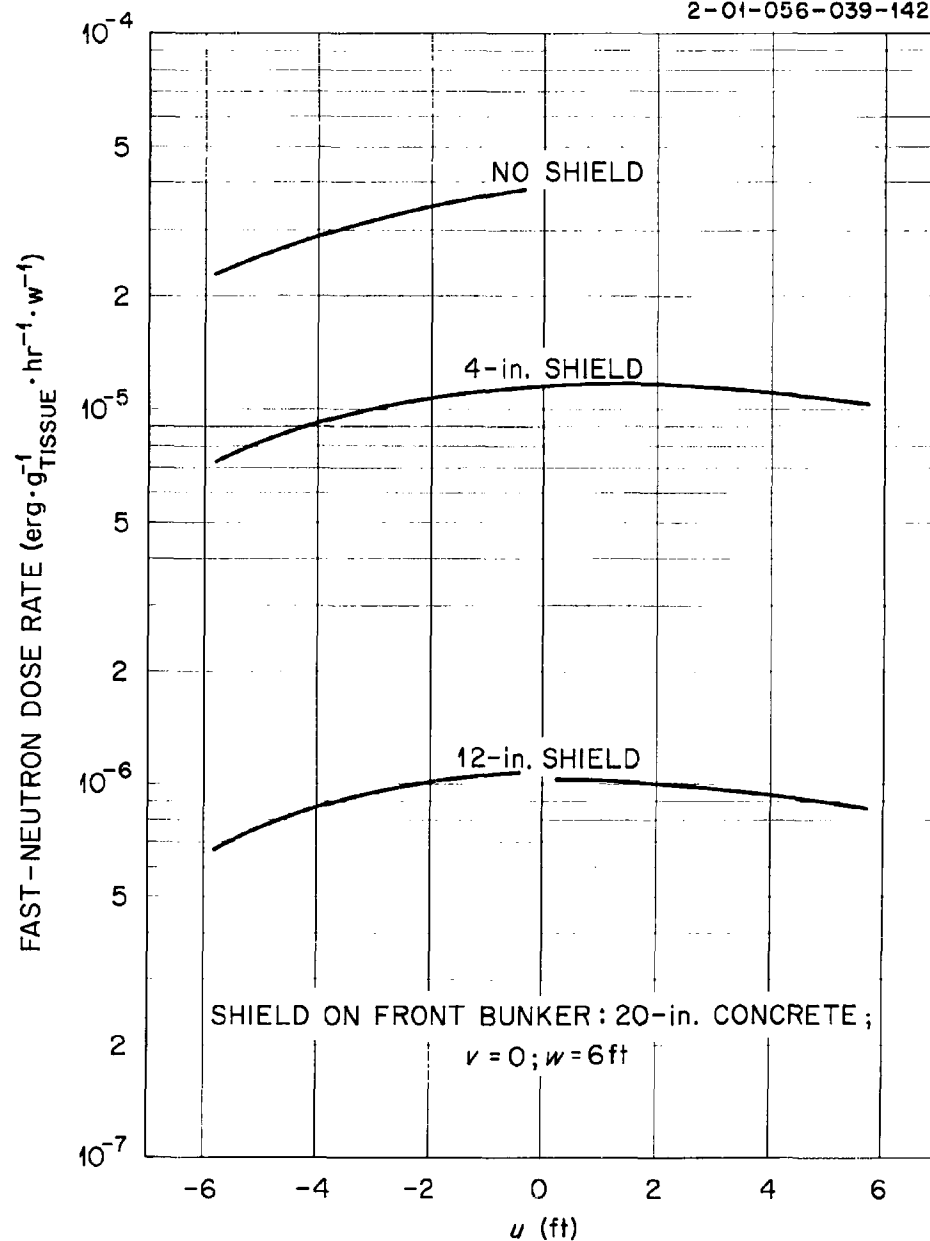


Fig. 16. Fast-Neutron Dose Rates in Top Bunker as a Function of  $u$  for Various Shield Thicknesses on the Top Face.

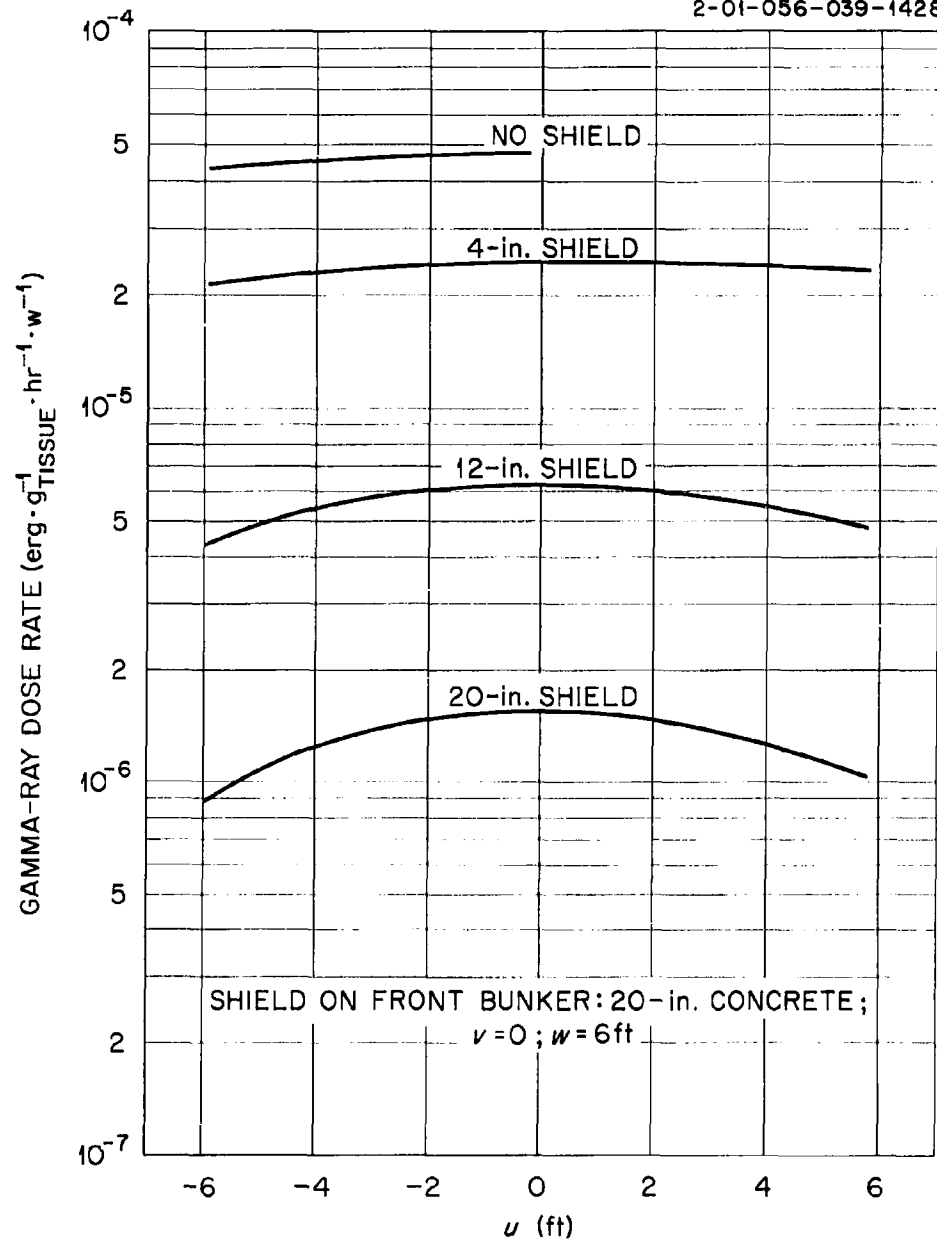
UNCLASSIFIED  
2-01-056-039-1428

Fig. 17. Gamma-Ray Dose Rates in Top Bunker as a Function of  $u$  for Various Shield Thicknesses on the Top Face.



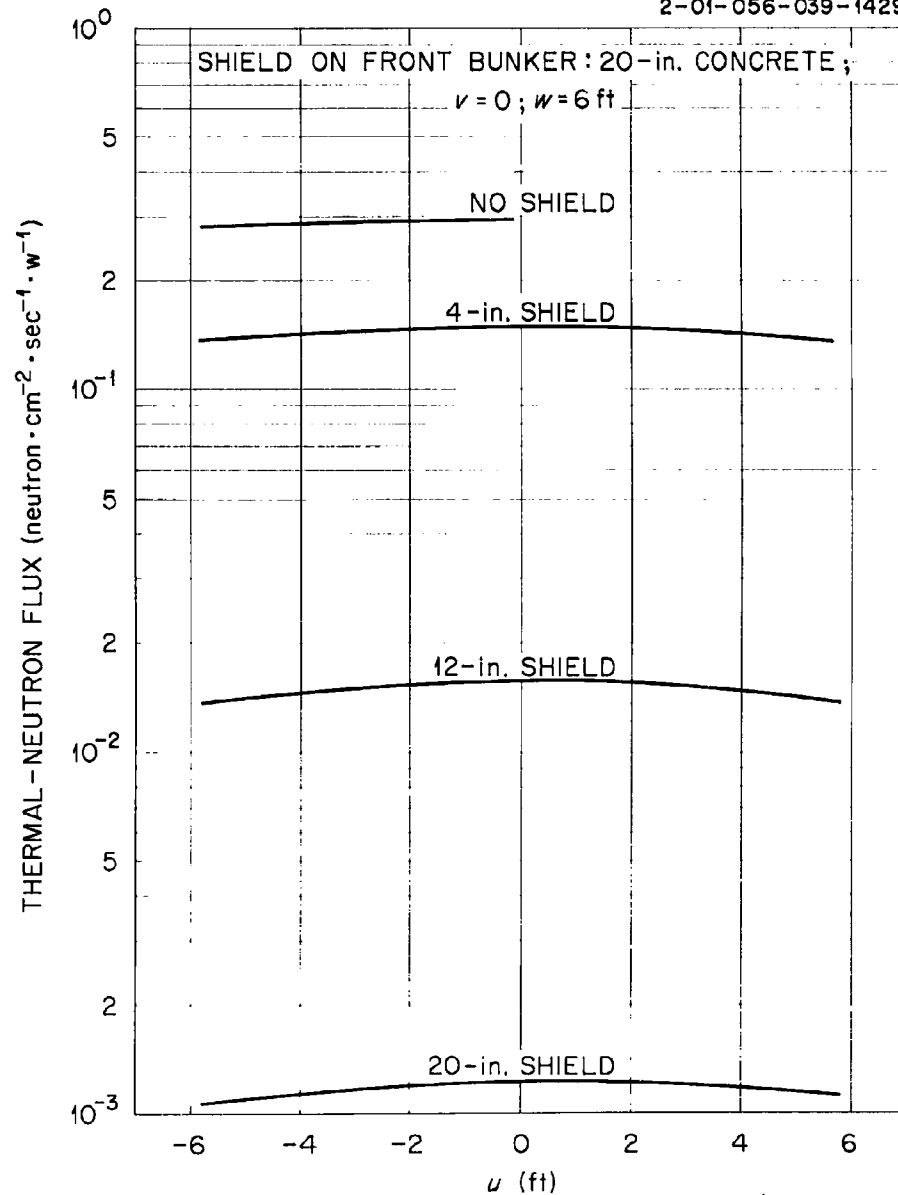
UNCLASSIFIED  
2-01-056-039-1429

Fig. 18. Thermal-Neutron Fluxes in Top Bunker as a Function of  $u$  for Various Shield Thicknesses on the Top Face.

UNCLASSIFIED  
2-01-056-039-1430

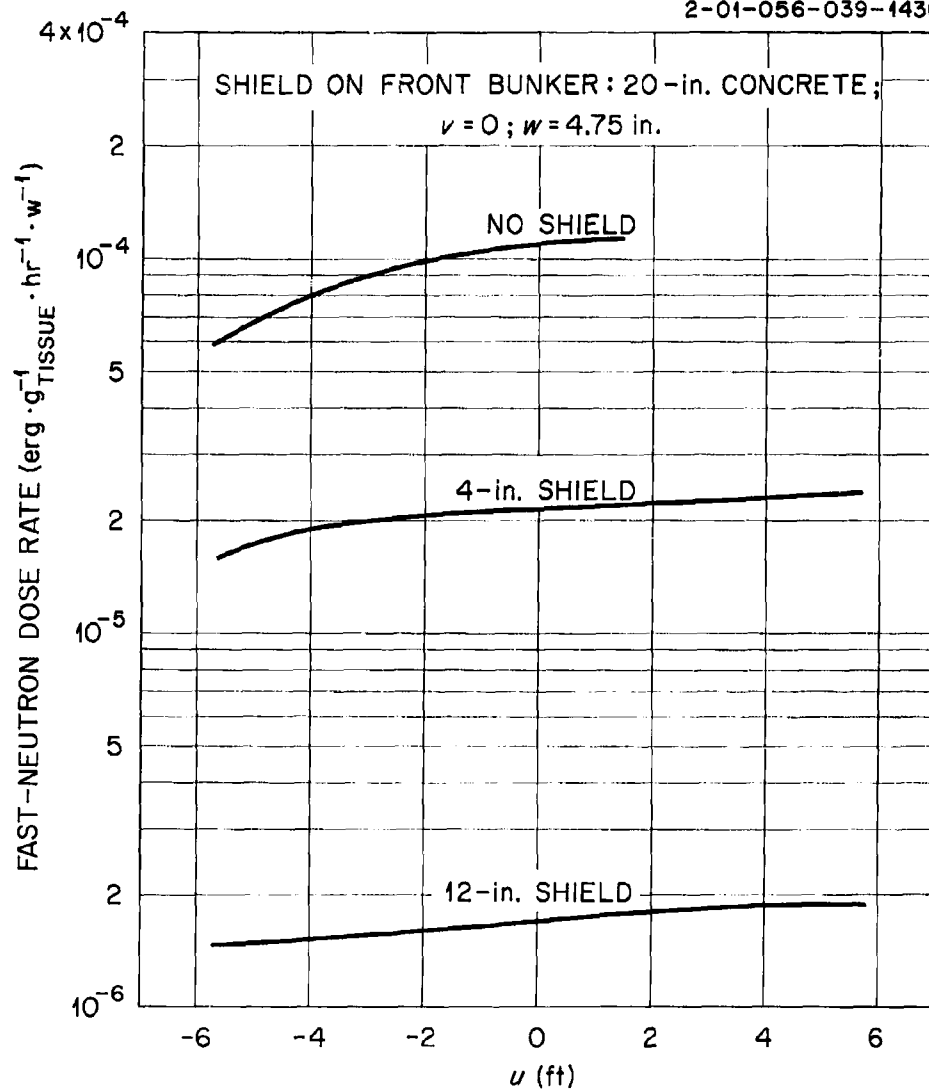


Fig. 19. Fast-Neutron Dose Rates in Top Bunker as a Function of  $u$  for Various Shield Thicknesses on the Top Face.

UNCLASSIFIED  
2-01-056-039-1431

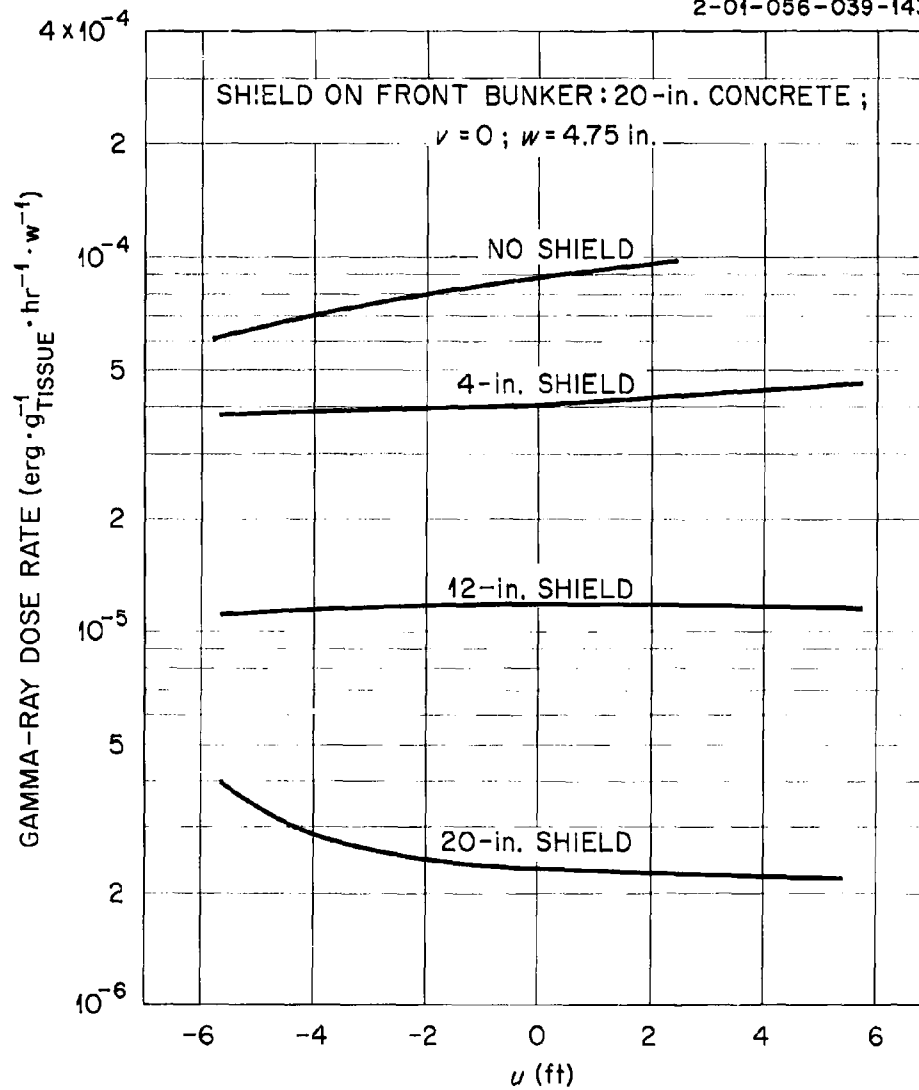


Fig. 20. Gamma-Ray Dose Rates in Top Bunker as a Function of  $u$  for Various Shield Thicknesses on the Top Face.

UNCLASSIFIED  
2-01-056-039-1432

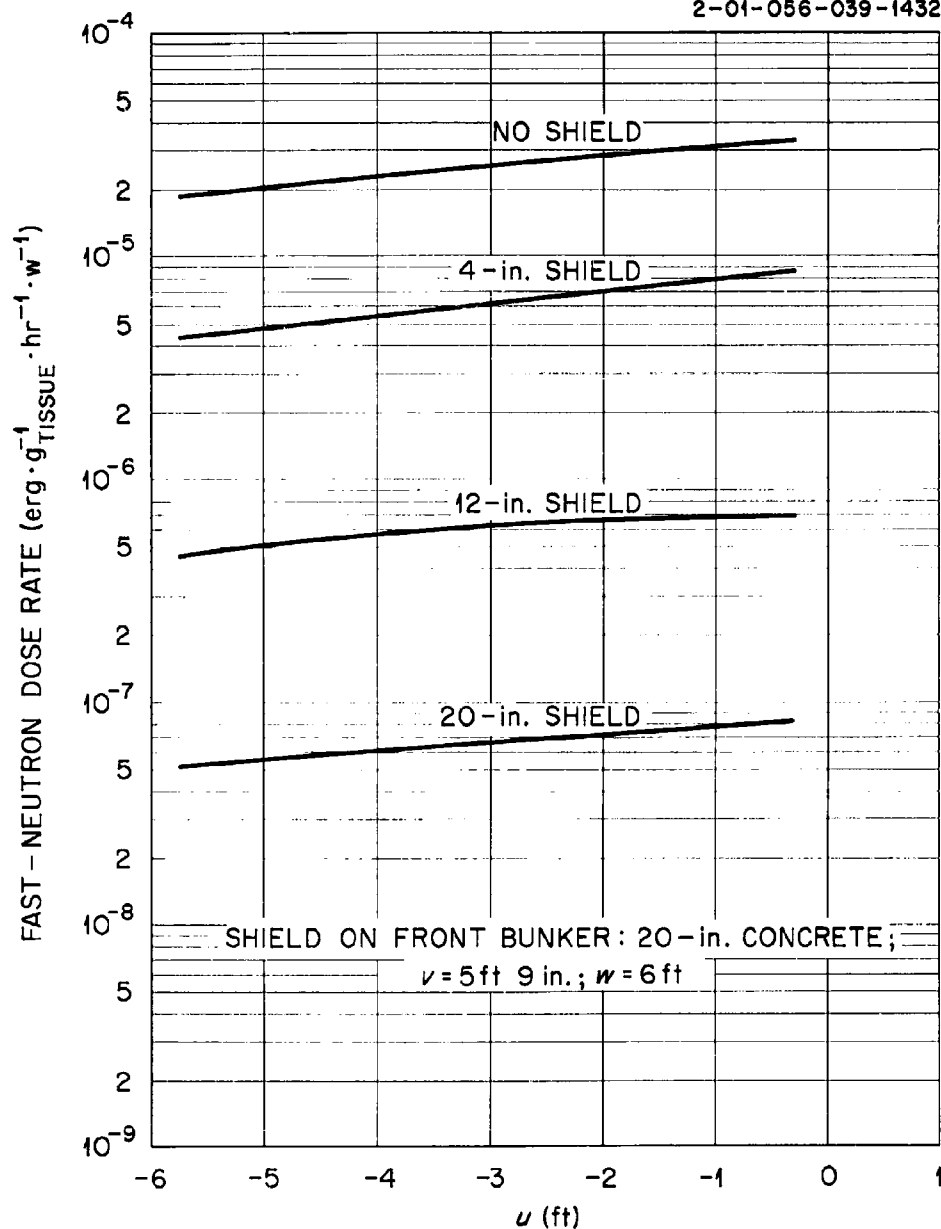


Fig. 21. Fast-Neutron Dose Rates in Top Bunker as a Function of  $u$  for Various Shield Thicknesses on the Top Face.

UNCLASSIFIED  
2-01-056-039-1433

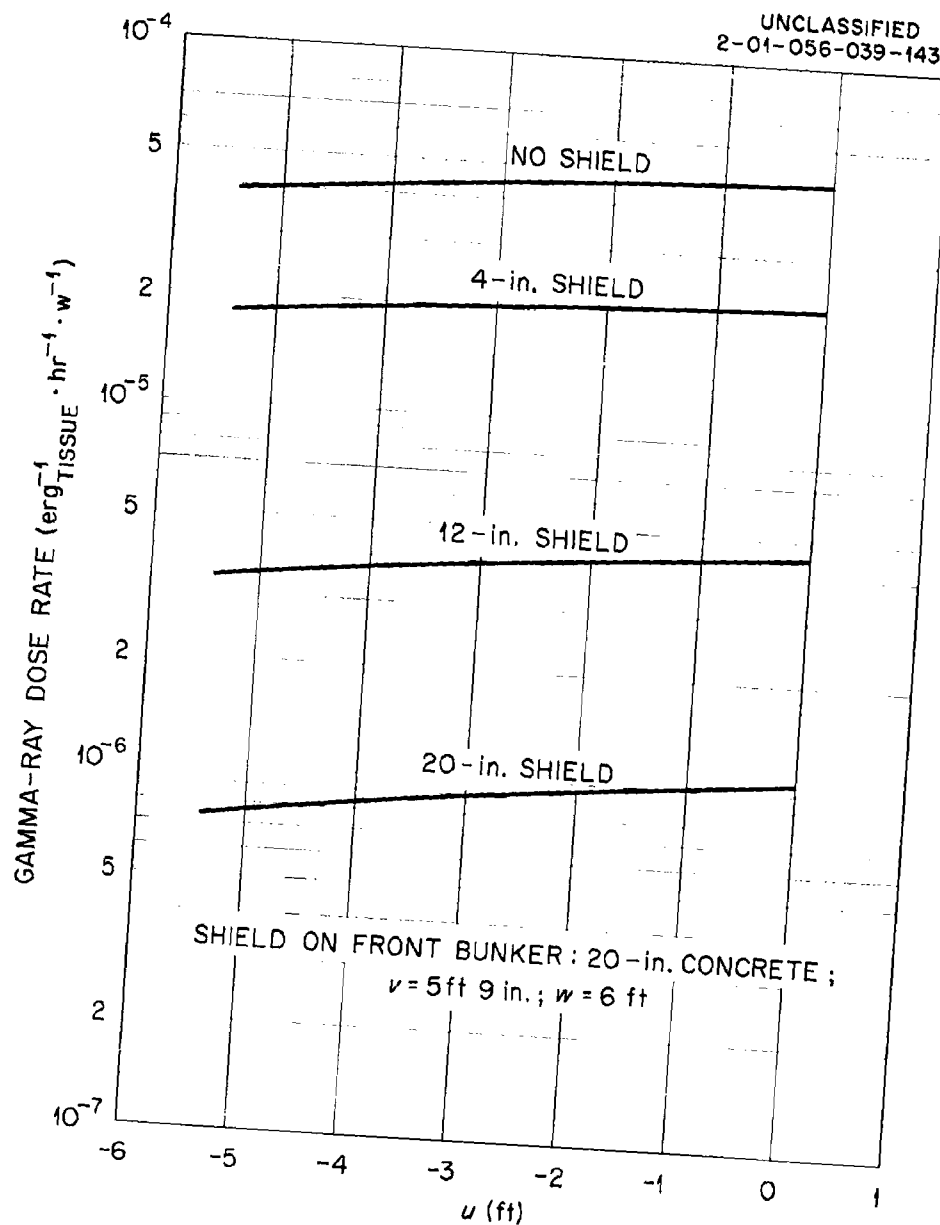


Fig. 22. Gamma-Ray Dose Rates in Top Bunker as a Function of  $u$  for Various Shield Thicknesses on the Top Face.

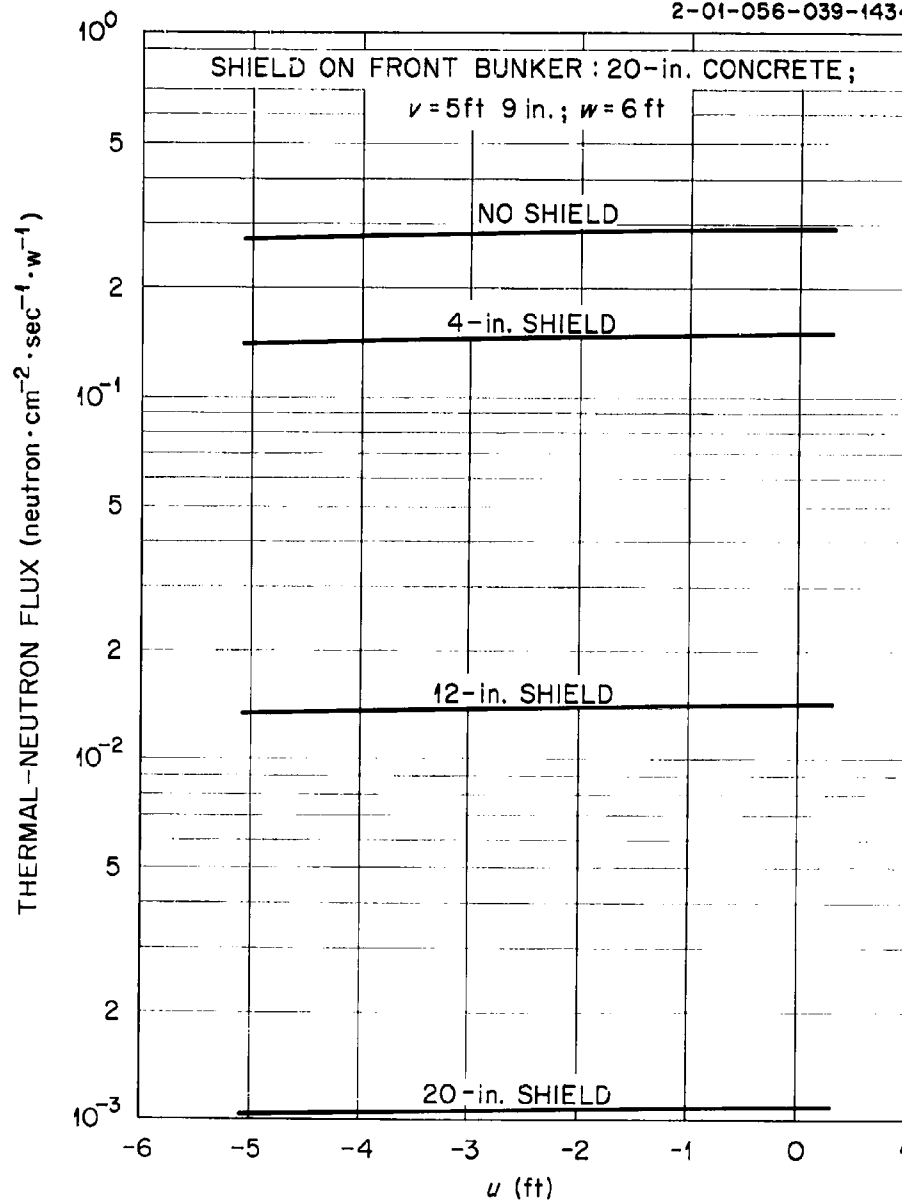
UNCLASSIFIED  
2-01-056-039-1434

Fig. 23. Thermal-Neutron Fluxes in Top Bunker as a Function of  $u$  for Various Shield Thicknesses on the Top Face.

UNCLASSIFIED  
2-01-056-039-1435

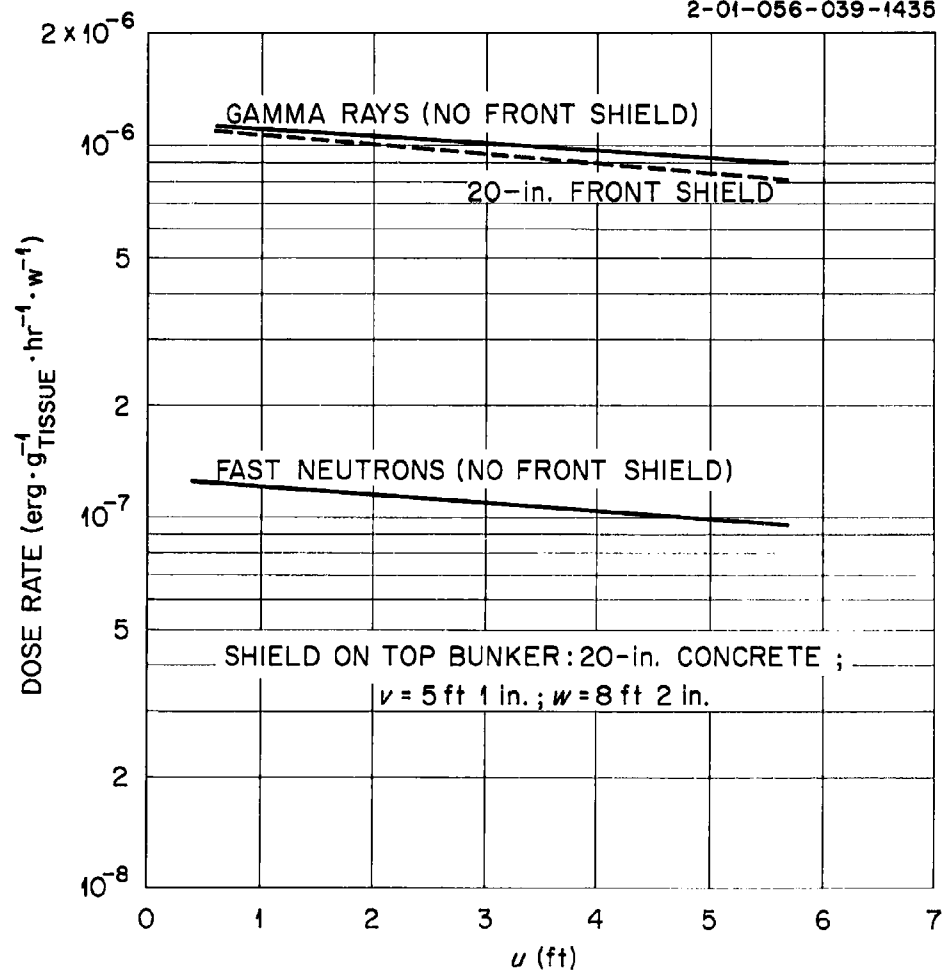


Fig. 24. Fast-Neutron and Gamma-Ray Dose Rates in Top Bunker Near Opening to Interconnecting Tunnel.

UNCLASSIFIED  
2-01-056-039-1436

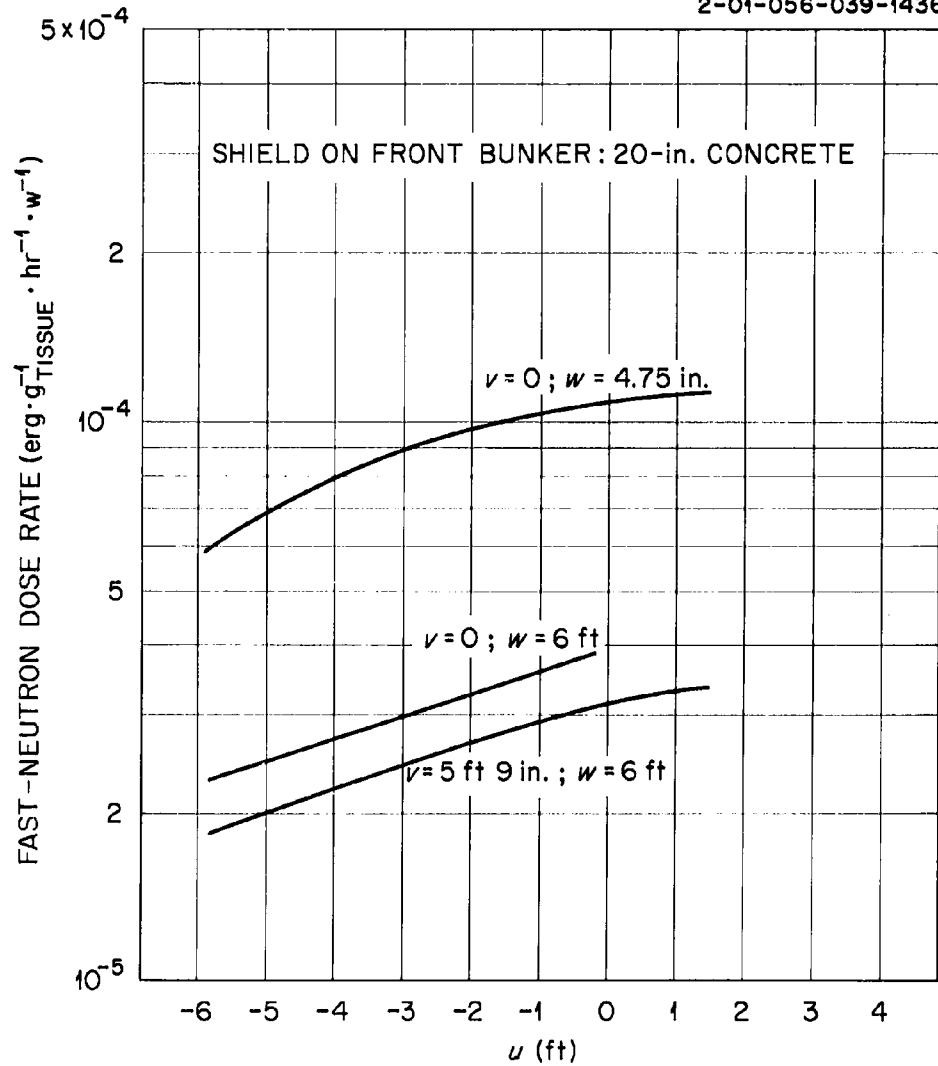


Fig. 25. Fast-Neutron Dose Rates in Top Bunker with No Top Shield as a Function of  $u$  for Various Values of  $v$  and  $w$ .



UNCLASSIFIED  
2-01-056-039-1437

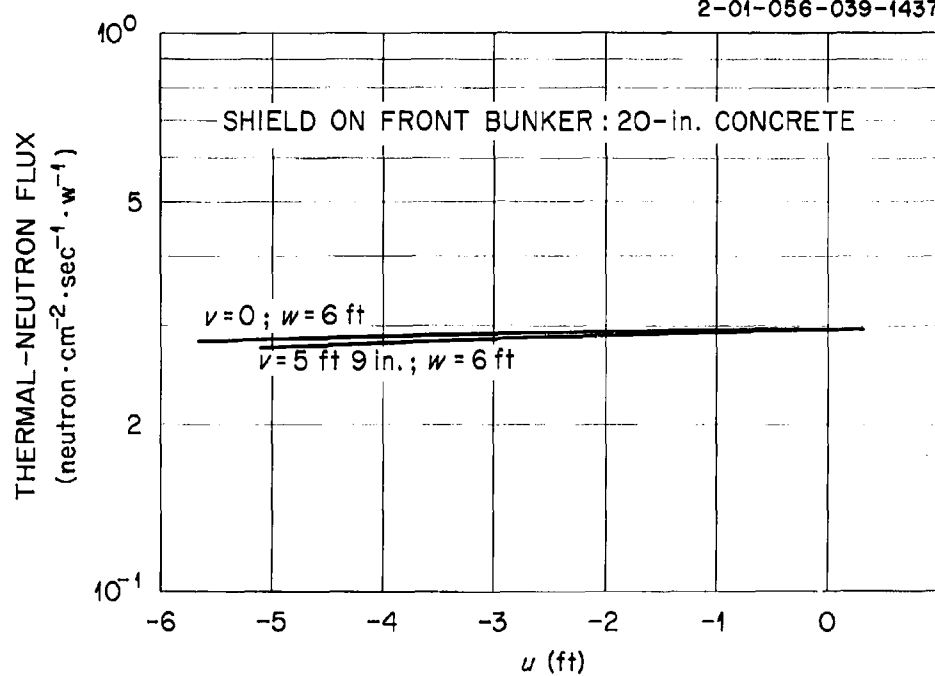


Fig. 26. Thermal-Neutron Fluxes in Top Bunker with No Top Shield as a Function of  $u$  for Various Values of  $v$  and  $w$ .

UNCLASSIFIED  
2-01-056-039-1438

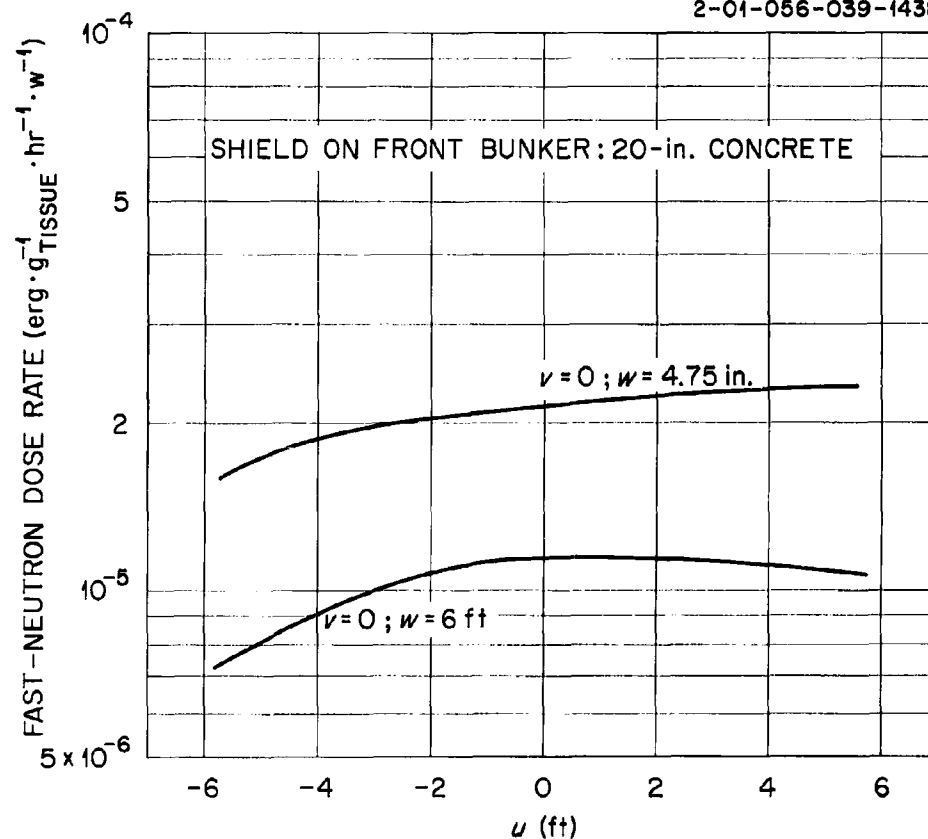


Fig. 27. Fast-Neutron Dose Rates in Top Bunker with 4-in. Top Shield as a Function of  $u$  for Various Values of  $w$ .

UNCLASSIFIED  
2-01-056-039-1439

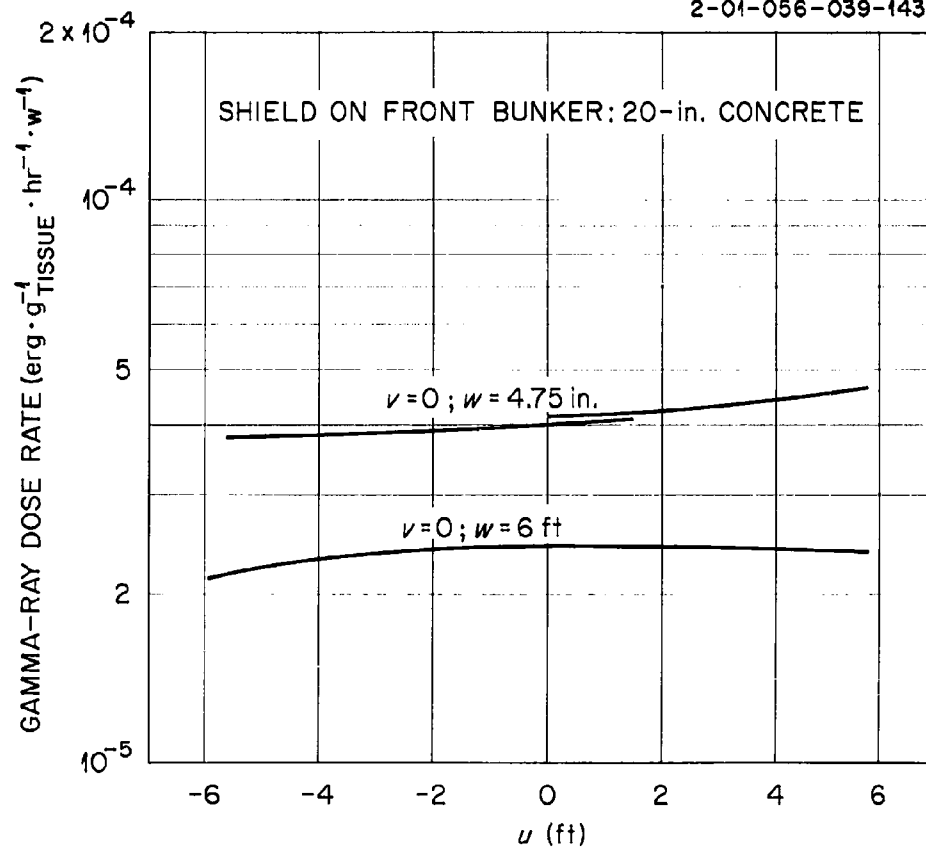


Fig. 28. Gamma-Ray Dose Rates in Top Bunker with 4-in. Top Shield as a Function of  $u$  for Various Values of  $w$ .

UNCLASSIFIED  
2-01-056-039-1440

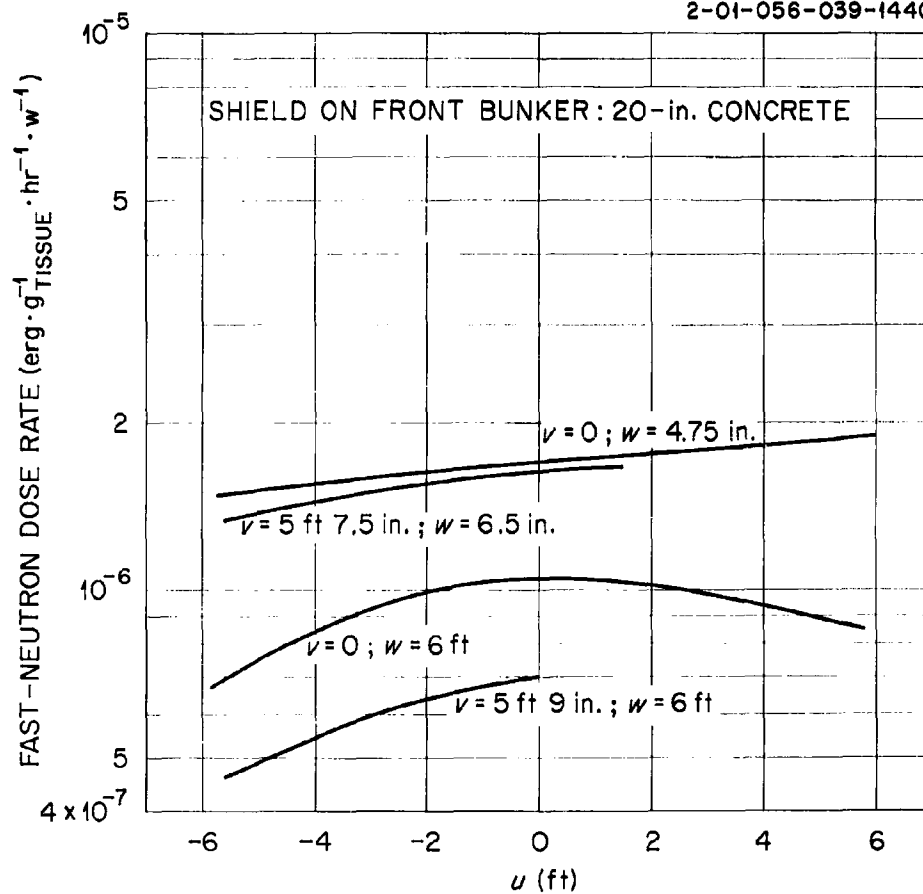


Fig. 29. Fast-Neutron Dose Rates in Top Bunker with 12-in. Top Shield as a Function of  $u$  for Various Values of  $v$  and  $w$ .

UNCLASSIFIED  
2-01-056-039-1441

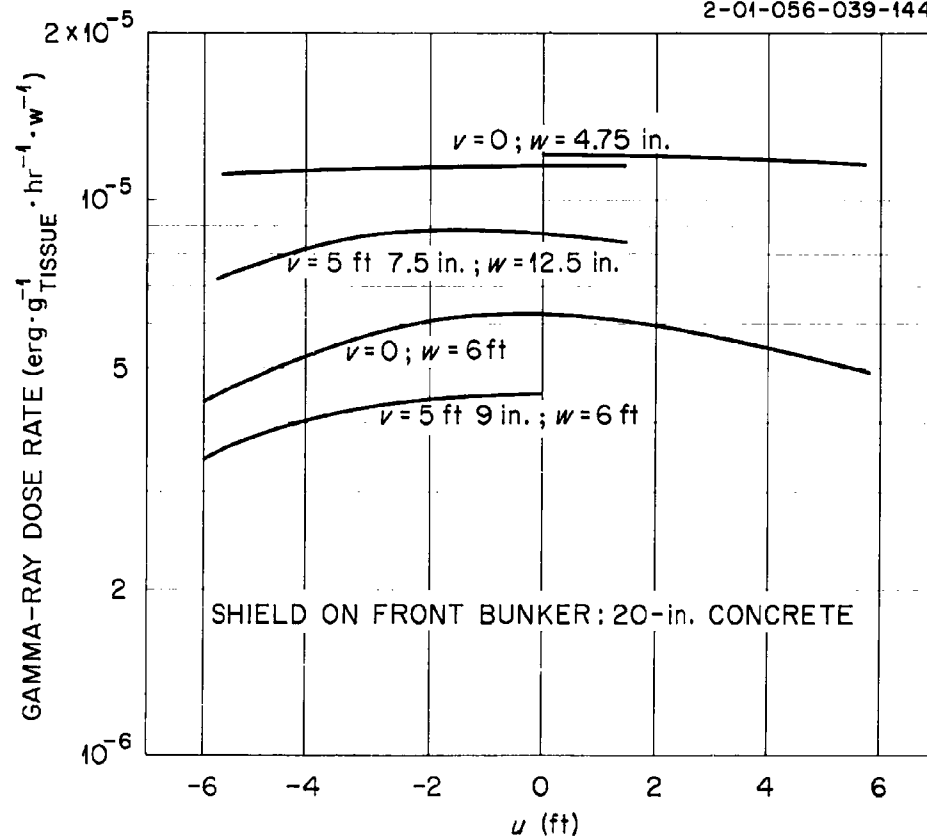


Fig. 30. Gamma-Ray Dose Rates in Top Bunker with 12-in. Top Shield as a Function of  $u$  for Various Values of  $v$  and  $w$ .

UNCLASSIFIED  
2-01-056-039-1442

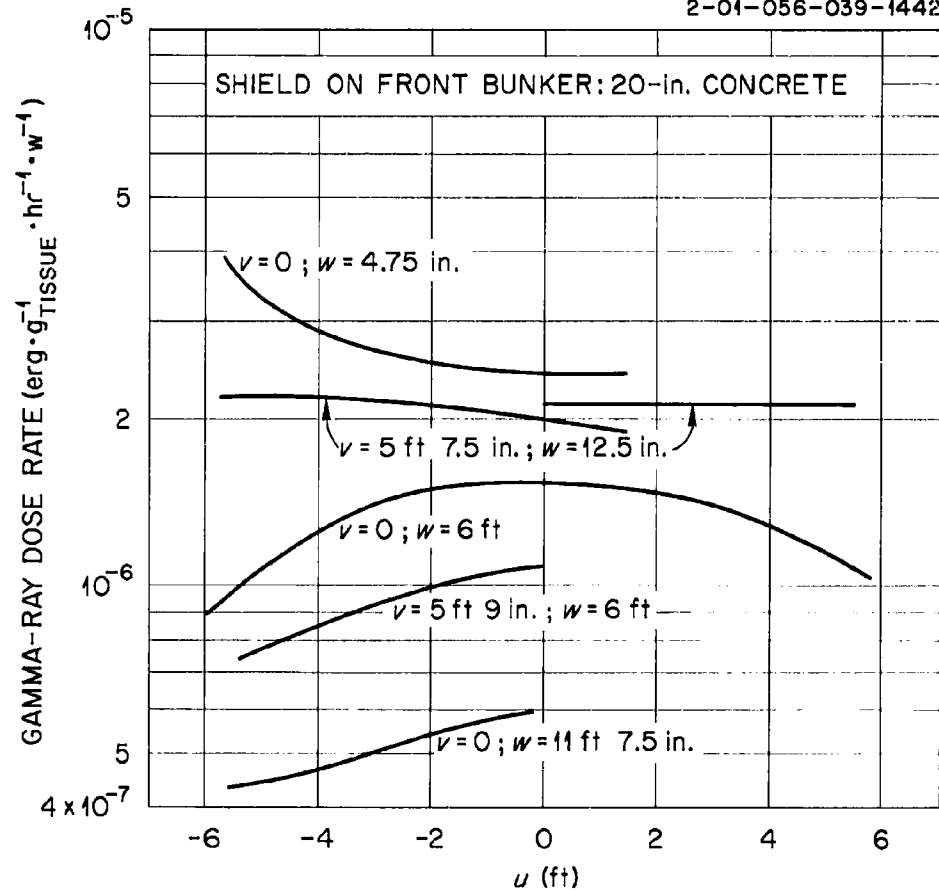


Fig. 31. Gamma-Ray Dose Rates in Top Bunker with 20-in. Top Shield as a Function of  $u$  for Various Values of  $v$  and  $w$ .

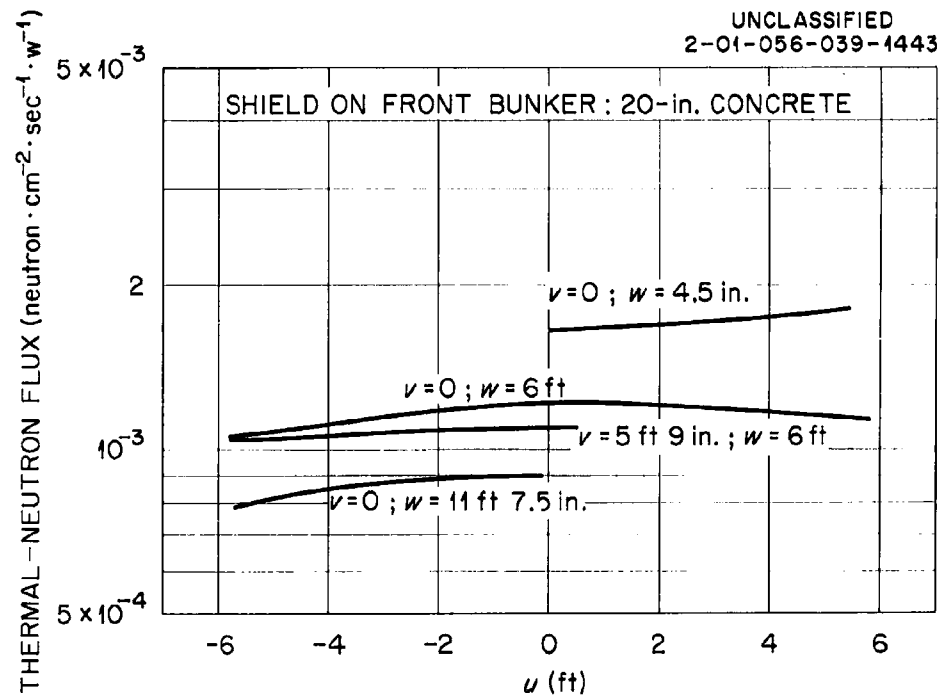


Fig. 32. Thermal-Neutron Fluxes in Top Bunker with 20-in. Top Shield as a Function of  $u$  for Various Values of  $v$  and  $w$ .

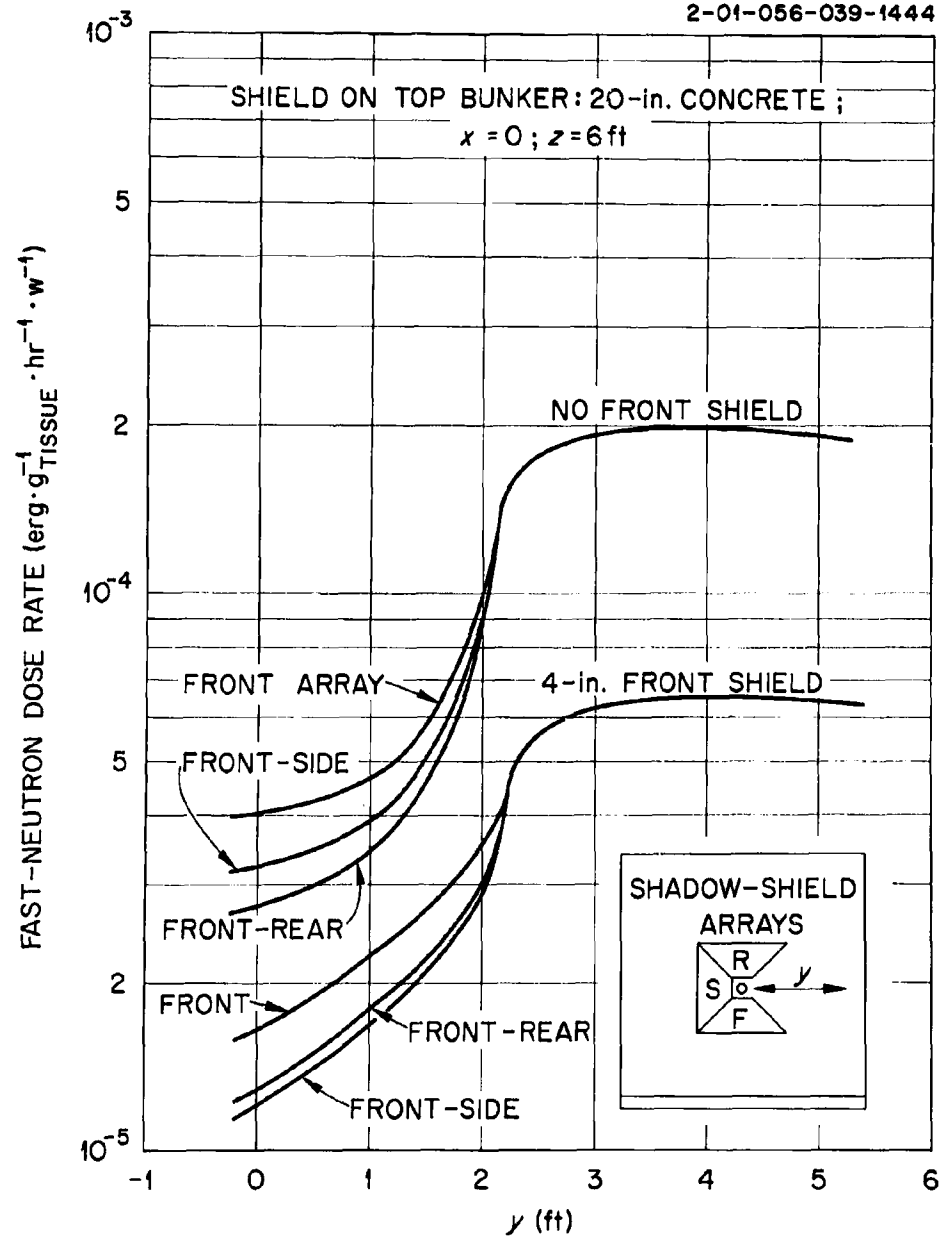
UNCLASSIFIED  
2-01-056-039-1444

Fig. 33. Fast-Neutron Dose Rates in Front Bunker as a Function of  $y$  for Various Shadow-Shield Arrangements.



UNCLASSIFIED  
2-01-056-039-1445

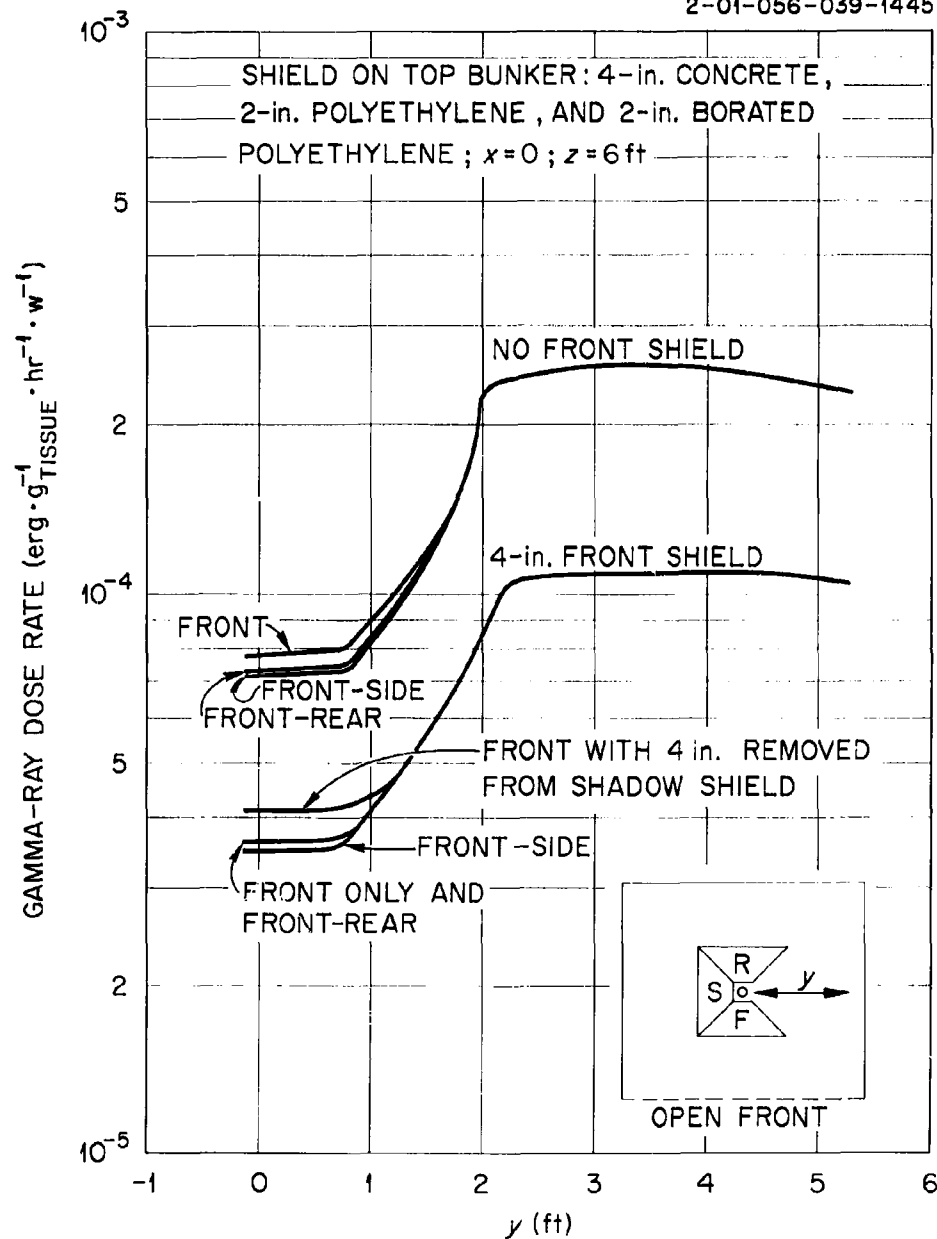


Fig. 34. Gamma-Ray Dose Rates in Front Bunker as a Function of  $y$  for Various Shadow-Shield Arrangements.

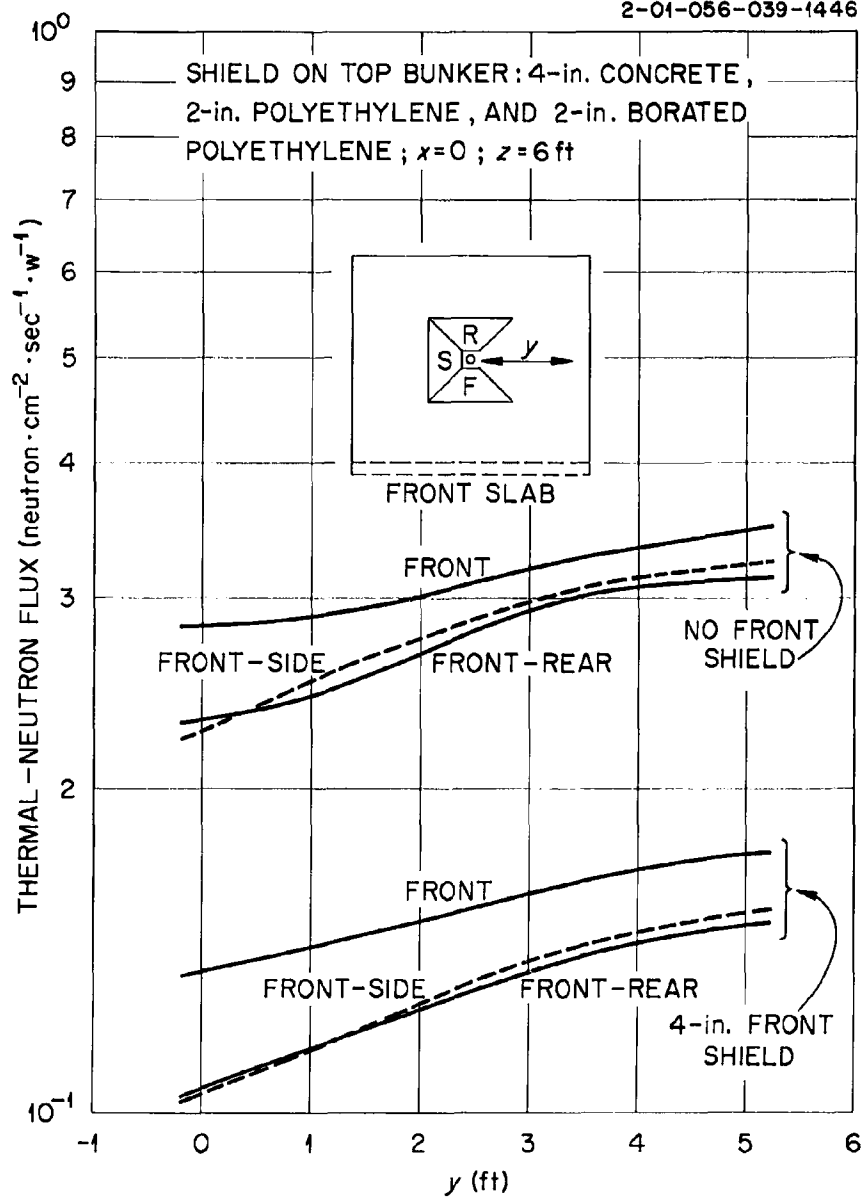
UNCLASSIFIED  
2-01-056-039-1446

Fig. 35. Thermal-Neutron Fluxes in Front Bunker as a Function of  $y$  for Various Shadow-Shield Arrangements.

UNCLASSIFIED  
2-01-056-039-1447

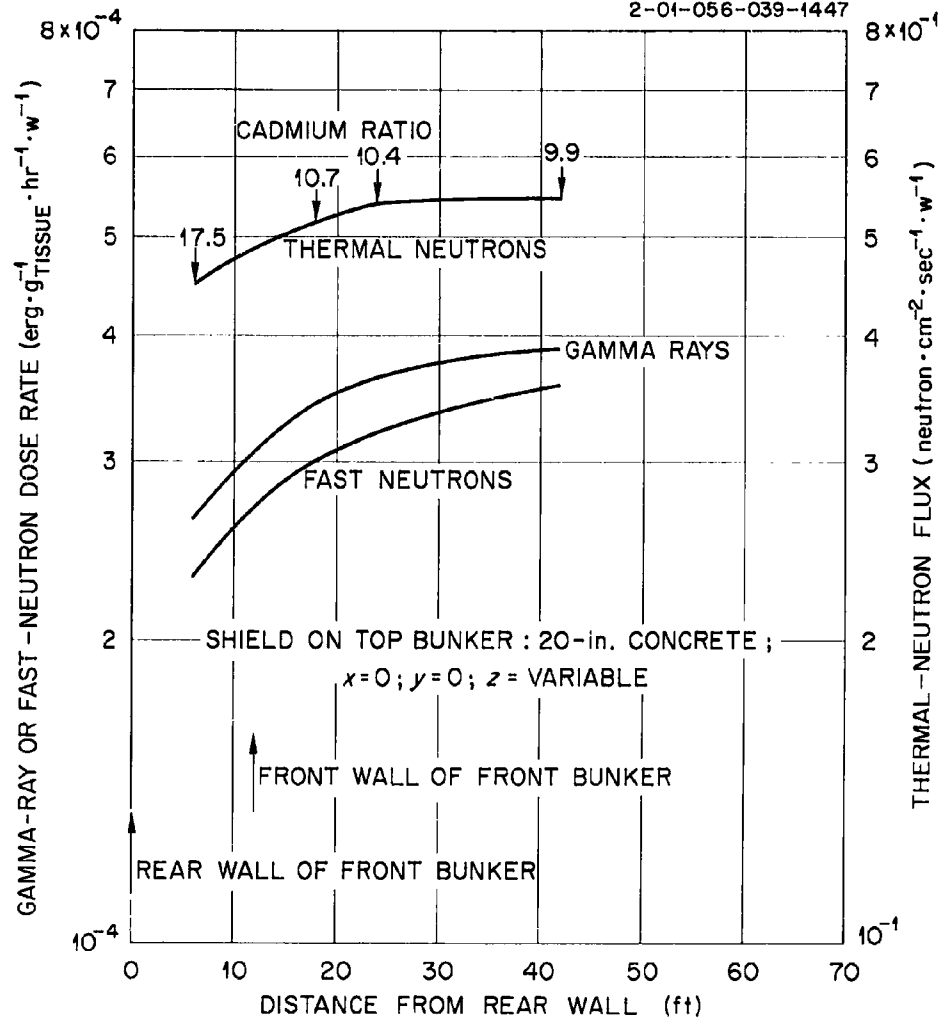


Fig. 36. Fast-Neutron and Gamma-Ray Dose Rates and Thermal-Neutron Fluxes Along  $z$  Axis of Front Bunker, Extending from Rear Wall to 30 ft in Front of Bunker (No Shield on Front Face).

UNCLASSIFIED  
2-01-056-039-1448

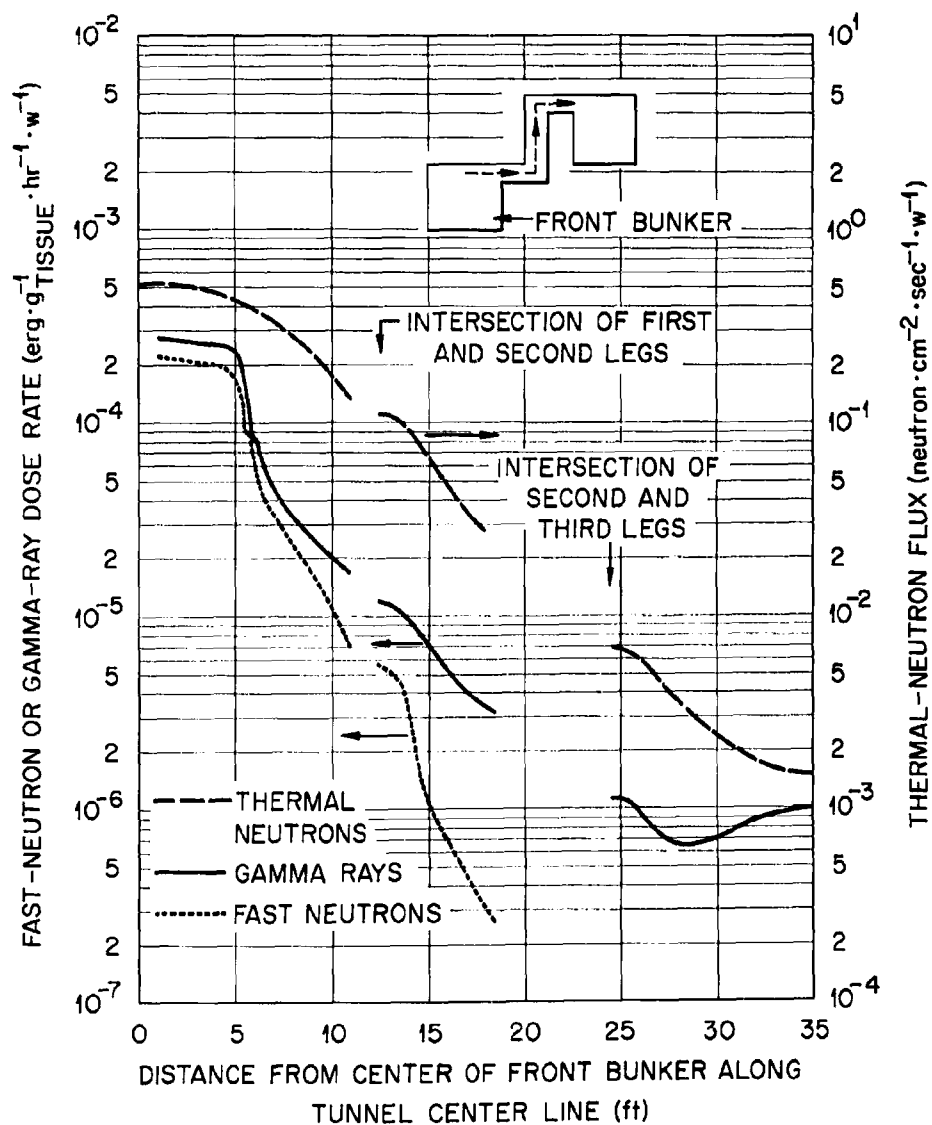


Fig. 37. Fast-Neutron and Gamma-Ray Dose Rates and Thermal-Neutron Fluxes Along Center Line of Interconnecting Tunnel for 20-in. Top Shield and No Front Shield.

UNCLASSIFIED  
2-01-056-039-1449

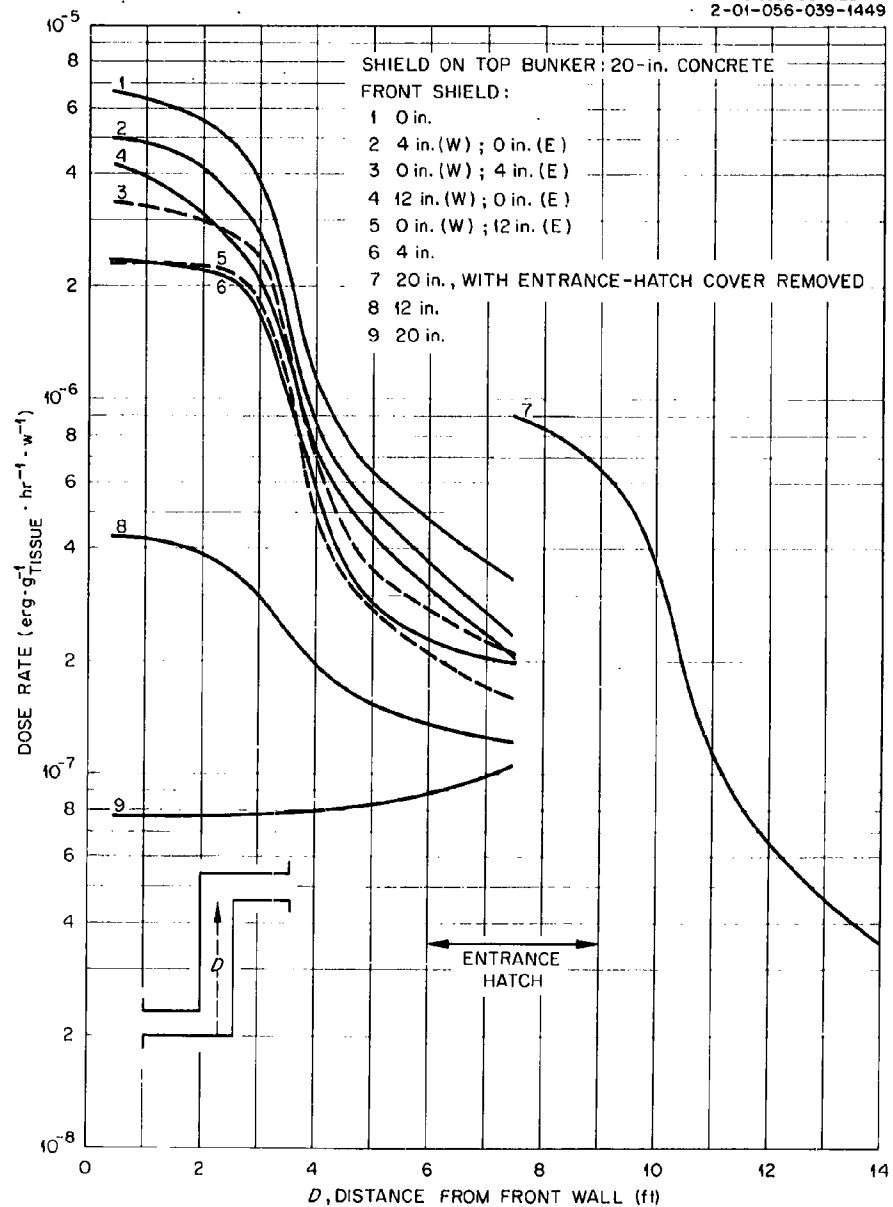


Fig. 38. Fast-Neutron Dose Rates Along Center Line of Middle Leg of Interconnecting Tunnel for Various Shield Thicknesses on Front Bunker.

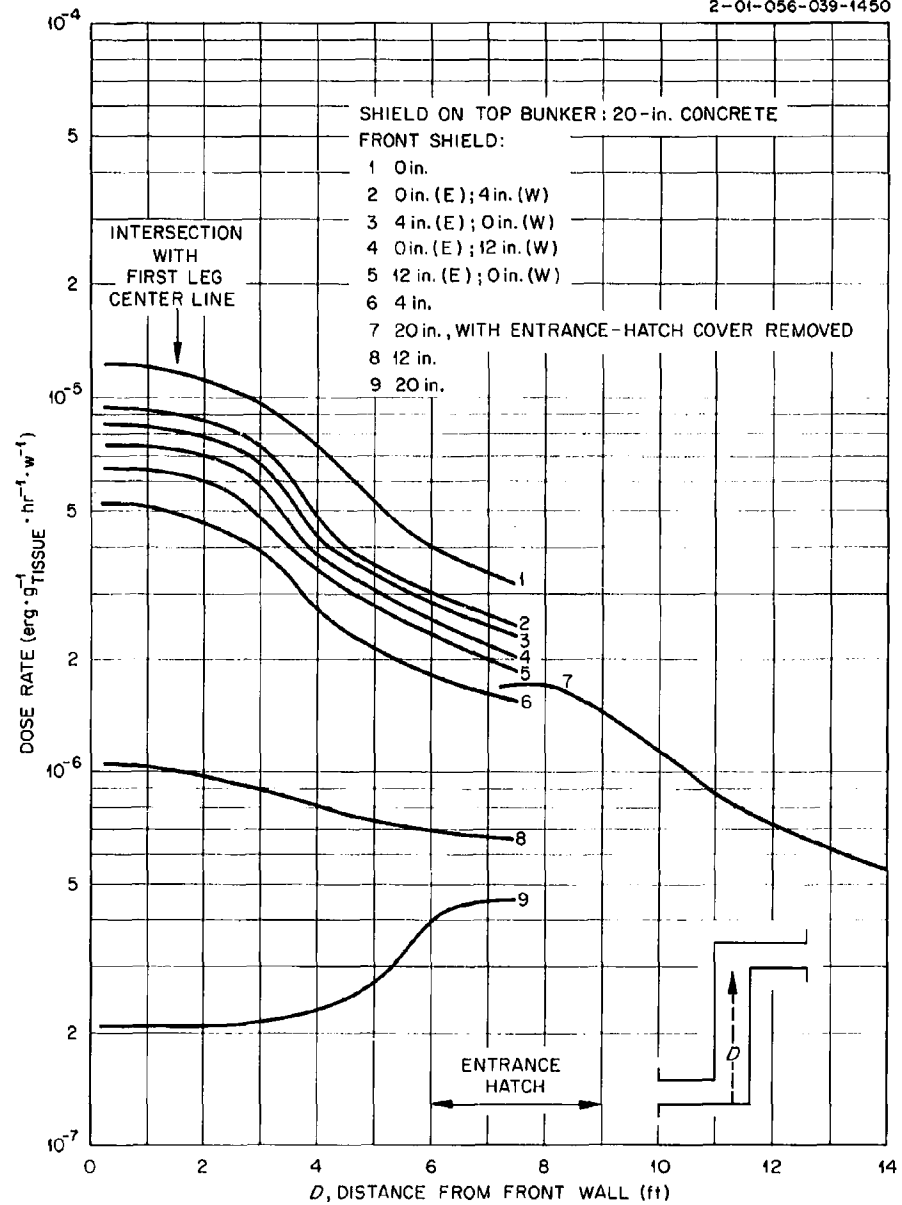
UNCLASSIFIED  
2-01-056-039-1450

Fig. 39. Gamma-Ray Dose Rates Along Center Line of Middle Leg of Interconnecting Tunnel for Various Shield Thicknesses on Front Bunker.

UNCLASSIFIED  
2-01-056-039-1451

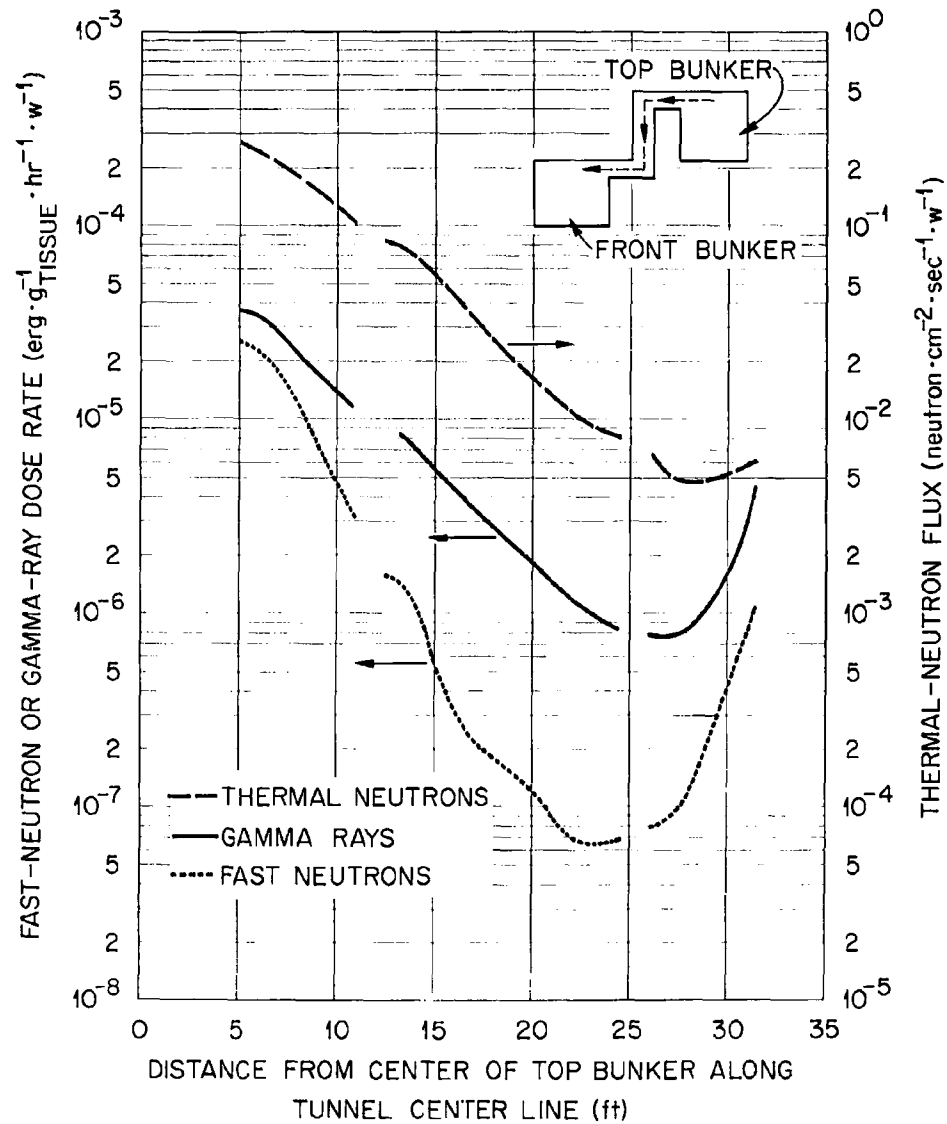


Fig. 40. Fast-Neutron and Gamma-Ray Dose Rates and Thermal-Neutron Fluxes Along Center Line of Interconnecting Tunnel for 20-in. Front Shield and No Top Shield.

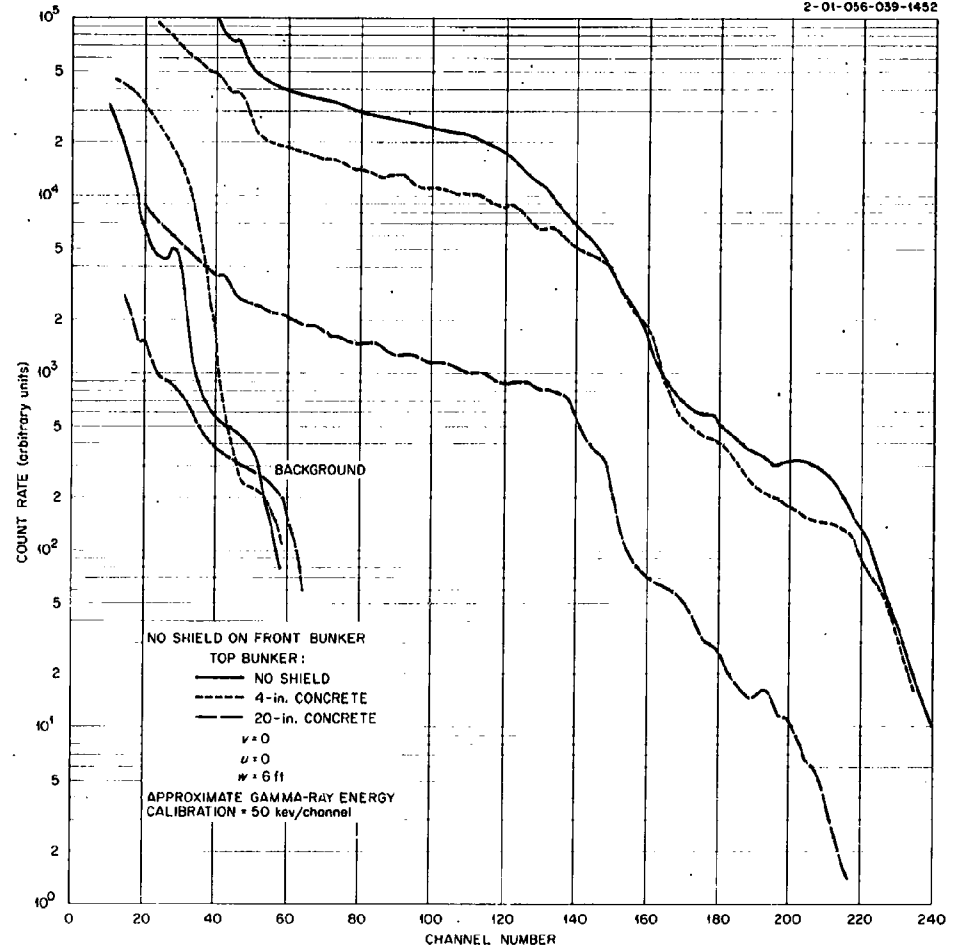
UNCLASSIFIED  
2-01-056-039-1452

Fig. 41. Gamma-Ray Pulse-Height Spectra in Center of Top Bunker for Top Shields of 0, 4, and 20 in. of Concrete.



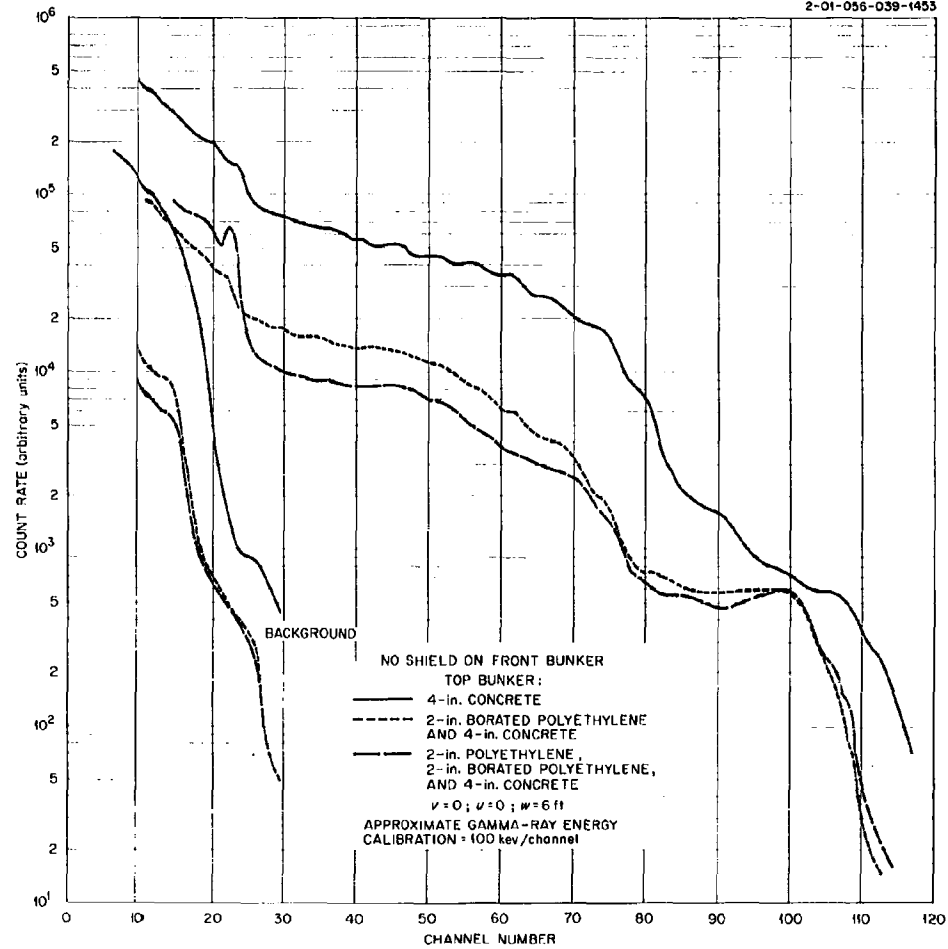
UNCLASSIFIED  
2-01-056-039-1453

Fig. 42. Gamma-Ray Pulse-Height Spectra in Center of Top Bunker for Various Top Shields of Concrete and Borated Polyethylene.

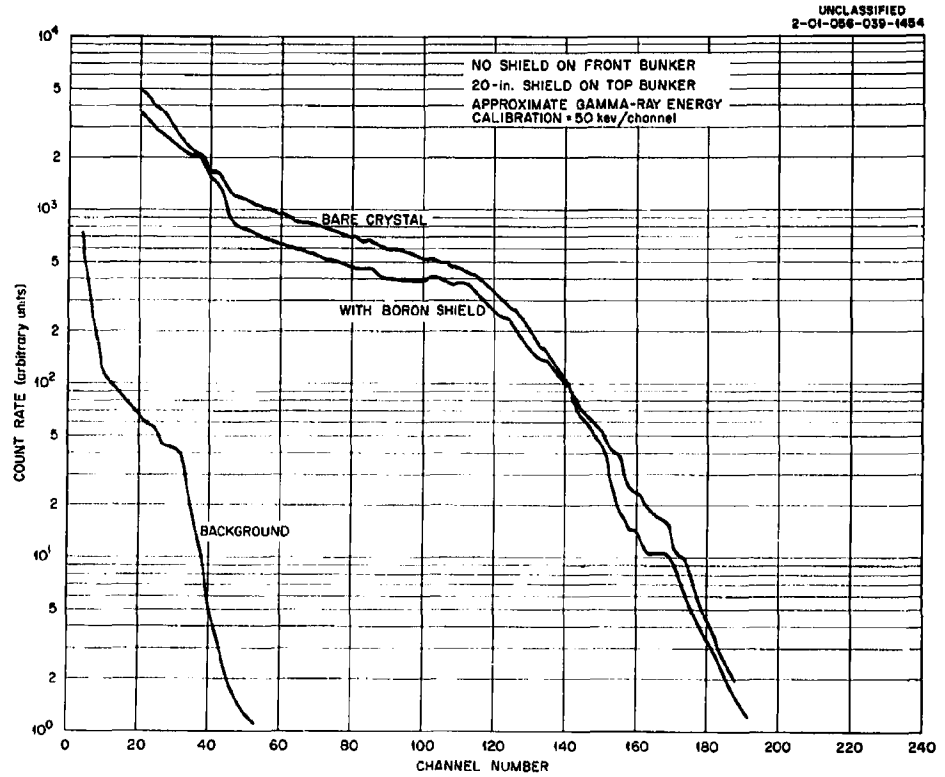


Fig. 43. Gamma-Ray Pulse-Height Spectra in Center of Tunnel, With and Without Boron on Crystal.

## LIST OF FIGURES.

<u>Fig. No.</u>		<u>Page No.</u>
1	Tower Shielding Facility -----	2
2	Location of Concrete Bunkers and Tunnels -----	3
3	TSR-II Shields COOL-I and COOL-II -----	5
4	Neutron-Leakage Spectra of TSR-II Shields -----	6
5	Schematic of Bunker-Tunnel Arrangement, Showing the Coordinate Systems -----	7
6	Investigation of Effect of Thermal-Neutron Response of Anthracene Crystal: Gamma-Ray Dose Rates in Second and Third Legs of Tunnel With and Without $Li^6$ Shield Surrounding Crystal -----	10
7	Fast-Neutron Dose Rates in Front and Top Bunkers as a Function of Reactor Altitude -----	12
8	Gamma-Ray Dose Rates in Front and Top Bunkers as a Function of Reactor Altitude -----	13
9	Fast-Neutron Dose Rates Along z Axis of Front Bunker for Various Shield Thicknesses on the Front Face -----	25
10	Gamma-Ray Dose Rates Along z Axis of Front Bunker for Various Shield Thicknesses on the Front Face -----	26
11	Thermal-Neutron Fluxes Along z Axis of Front Bunker for Various Shield Thicknesses on the Front Face -----	27
12	Fast-Neutron and Gamma-Ray Dose Rates in Front Bunker as a Function of z Position for Various x and y Values -----	28
13	Fast-Neutron Dose Rates Along w Axis of Top Bunker for Various Shield Thicknesses on the Top Face -----	29
14	Gamma-Ray Dose Rates Along w Axis of Top Bunker for Various Shield Thicknesses on the Top Face -----	30
15	Thermal-Neutron Fluxes Along w Axis of Top Bunker for Various Shield Thicknesses on the Top Face -----	31
16	Fast-Neutron Dose Rates in Top Bunker as a Function of u for Various Shield Thicknesses on the Top Face -----	32

<u>Fig. No.</u>		<u>Page No.</u>
17	Gamma-Ray Dose Rates in Top Bunker as a Function of u for Various Shield Thicknesses on the Top Face -----	33
18	Thermal-Neutron Fluxes in Top Bunker as a Function of u for Various Shield Thicknesses on the Top Face -----	34
19	Fast-Neutron Dose Rates in Top Bunker as a Function of u for Various Shield Thicknesses on the Top Face -----	35
20	Gamma-Ray Dose Rates in Top Bunker as a Function of u for Various Shield Thicknesses on the Top Face -----	36
21	Fast-Neutron Dose Rates in Top Bunker as a Function of u for Various Shield Thicknesses on the Top Face -----	37
22	Gamma-Ray Dose Rates in Top Bunker as a Function of u for Various Shield Thicknesses on the Top Face. -----	38
23	Thermal-Neutron Fluxes in Top Bunker as a Function of u for Various Shield Thicknesses on the Top Face -----	39
24	Fast-Neutron and Gamma-Ray Dose Rates in Top Bunker Near Opening to Interconnecting Tunnel -----	40
25	Fast-Neutron Dose Rates in Top Bunker with No Top Shield as a Function of u for Various Values of v and w -----	41
26	Thermal-Neutron Fluxes in Top Bunker with No Top Shield as a Function of u for Various Values of v and w -----	42
27	Fast-Neutron Dose Rates in Top Bunker with 4-in. Top Shield as a Function of u for Various Values of w -----	43
28	Gamma-Ray Dose Rates in Top Bunker with 4-in. Top Shield as a Function of u for Various Values of w -----	44
29	Fast-Neutron Dose Rates in Top Bunker with 12-in. Top Shield as a Function of u for Various Values of v and w -----	45
30	Gamma-Ray Dose Rates in Top Bunker with 12-in. Top Shield as a Function of u for Various Values of v and w -----	46
31	Gamma-Ray Dose Rates in Top Bunker with 20-in. Top Shield as a Function of u for Various Values of v and w -----	47

<u>Fig. No.</u>		<u>Page No.</u>
32	Thermal-Neutron Fluxes in Top Bunker with 20-in. Top Shield as a Function of u for Various Values of v and w -----	48
33	Fast-Neutron Dose Rates in Front Bunker as a Function of y for Various Shadow-Shield Arrangements -----	49
34	Gamma-Ray Dose Rates in Front Bunker as a Function of y for Various Shadow-Shield Arrangements -----	50
35	Thermal-Neutron Fluxes in Front Bunker as a Function of y for Various Shadow-Shield Arrangements -----	51
36	Fast-Neutron and Gamma-Ray Dose Rates and Thermal-Neutron Fluxes Along z Axis of Front Bunker, Extending from Rear Wall to 30 ft in Front of Bunker (No Shield on Front Face) -----	52
37	Fast-Neutron and Gamma-Ray Dose Rates and Thermal-Neutron Fluxes Along Center Line of Interconnecting Tunnel for 20-in. Top Shield and No Front Shield -----	53
38	Fast-Neutron Dose Rates Along Center Line of Middle Leg of Interconnecting Tunnel for Various Shield Thicknesses on Front Bunker -----	54
39	Gamma-Ray Dose Rates Along Center Line of Middle Leg of Interconnecting Tunnel for Various Shield Thicknesses on Front Bunker -----	55
40	Fast-Neutron and Gamma-Ray Dose Rates and Thermal-Neutron Fluxes Along Center Line of Interconnecting Tunnel for 20-in. Front Shield and No Top Shield -----	56
41	Gamma-Ray Pulse-Height Spectra in Center of Top Bunker for Top Shields of 0, 4, and 20 in. of Concrete -----	57
42	Gamma-Ray Pulse-Height Spectra in Center of Top Bunker for Various Top Shields of Concrete and Borated Polyethylene -----	58
43	Gamma-Ray Pulse-Height Spectra in Center of Tunnel, With and Without Boron on Crystal -----	59

ORNL-3464  
 UC-34 - Physics  
 TID-4500 (24th ed.)

## INTERNAL DISTRIBUTION

- |                                     |                                   |
|-------------------------------------|-----------------------------------|
| 1. Biology Library                  | 78. C. E. Larson                  |
| 2-4. Central Research Library       | 79. T. A. Lewis                   |
| 5. Reactor Division Library         | 80. J. A. Martin                  |
| 6-7. ORNL - Y-12 Technical Library  | 81. J. M. Miller                  |
| Document Reference Section          | 82. J. P. Nichols                 |
| 8-57. Laboratory Records Department | 83. J. W. Paul                    |
| 58. Laboratory Records, ORNL R.C.   | 84. S. K. Penny                   |
| 59. J. A. Auxier                    | 85. A. M. Perry                   |
| 60. T. V. Blalock                   | 86. F. W. Sanders                 |
| 61. E. P. Blizard                   | 87. M. J. Skinner                 |
| 62. J. C. Bresee                    | 88. J. A. Swartout                |
| 63. R. D. Bundy                     | 89. M. L. Tobias                  |
| 64-69. V. R. Cain                   | 90. D. K. Trubey                  |
| 70. G. A. Cristy                    | 91. J. W. Wachter                 |
| 71. F. J. Davis                     | 92. A. M. Weinberg                |
| 72. B. E. Foster                    | 93. W. Zobel                      |
| 73. F. M. Glass                     | 94. R. A. Charpie (consultant)    |
| 74. H. M. Glen                      | 95. P. F. Gast (consultant)       |
| 75. F. F. Haywood                   | 96. M. L. Goldberger (consultant) |
| 76. J. T. Howe                      | 97. H. F. Taschek (consultant)    |
| 77. W. H. Jordan                    | 98. T. J. Thompson (consultant)   |

## EXTERNAL DISTRIBUTION

- 99-158. Office of Civil Defense, DoD, Pentagon, Attn: Director for Research, Washington, D.C.
- 159-161. Army Library, Civil Dense Unit, Pentagon, Washington, D.C.
162. Assistant Secretary of the Army (R&D), Attn: Assistant for Research, Washington, D.C.
163. Chief of Naval Research (Code 104), Department of the Navy, Washington, D.C.
164. Chief of Naval Operations (Op-C7T10), Department of the Navy, Washington, D.C.
165. Chief, Bureau of Naval Weapons (Code RRRE-5), Department of the Navy, Washington, D.C.
166. Chief, Bureau of Medicine and Surgery, Department of the Navy, Washington, D.C.
167. Chief, Bureau of Supplies and Accounts (Code 112), Department of the Navy, Washington, D.C.
168. Chief, Bureau of Yards and Docks, Office of Research (Code 74), Department of the Navy, Washington, D.C.
169. Commanding Officer and Director, U.S. Naval Civil Engineering Laboratory, Attn: Document Library, Port Hueneme, California
170. Advisory Committee on Civil Defense, National Academy of Sciences, Attn: Richard Park, 2101 Constitution Avenue, N.W., Washington, D.C.

Best Available Copy

- 171-190. Defense Documentation Center, Arlington Hall Station,  
Arlington, Virginia
- 191. Chief of Naval Personnel (Code Pers M12), Department of the  
Navy, Washington, D.C.
- 192. Coordinator, Marine Corps Landing Force, Development Activities,  
Quantico, Virginia
- 193. Director of Research and Development, Office of Emergency  
Planning, Washington, D.C.
- 194-195. Chief, Defense Atomic Support Agency, Attn: Document Library,  
Washington, D.C.
- 196-197. Chief, Defense Atomic Support Agency, Attn: Major F. A. Verser,  
Washington, D.C.
- 198. Ottawa University, Department of Physics, Attn: L. V. Spencer,  
Ottawa, Kansas
- 199. Principal Investigator, Office of Civil Defense, Contract  
OCD-OS-62-241, National Bureau of Standards, Washington, D.C.
- 200. Principal Investigator, Office of Civil Defense, Contract  
OCD-OS-62-145, Atomic Energy Commission, Oak Ridge, Tennessee
- 201. University of Illinois, Department of Civil Engineering,  
Attn: A. B. Chilton, Urbana, Illinois
- 202. Commanding Officer and Director, U.S. Naval Radiological  
Defense Laboratory, Attn: W. E. Kregar, San Francisco,  
California
- 203-204. Commanding Officer, U.S. Army Nuclear Defense Laboratory,  
Attn: H. Donnert and H. Tiller, Army Chemical Center, Edgewood,  
Maryland
- 205. Director, U.S. Army Ballistic Research Laboratory, Attn:  
F. Allen, Aberdeen Proving Ground, Maryland
- 206. Charles Eisenhauer, Neutrch Physics Division, Brookhaven  
National Laboratory, Upton, Long Island, New York
- 207. Kansas State University, Department of Nuclear Engineering,  
Attn: W. Kimel, Manhattan, Kansas
- 208. Director of the Reactor Facility, University of Virginia,  
Attn: T. C. Williamson, Charlottesville, Virginia
- 209-210. Chemical Laboratories, Defense Research Board, Attn: E. E.  
Massey and C. E. Clifford, Ottawa, Canada
- 211. A&M College of Texas, Department of Chemical Engineering,  
College Station, Texas
- 212. U.S. Naval Post Graduate School, Department of Physics, Attn:  
E. Milne, Monterey, California
- 213. University of Maryland, Department of Chemical Engineering,  
Attn: J. Silverman, College Park, Maryland
- 214. Commanding Officer and Director, U.S. Naval Civil Engineering  
Laboratory, Attn: C. M. Huddleston, Port Hueneme, California
- 215. Director, Civil Effects Test Group, Atomic Energy Commission,  
Attn: L. J. Deal, Washington, D.C.
- 216. Director, U.S. Army Materials Research Agency, Watertown  
Arsenal, Attn: Dorothy Weeks, Watertown, Massachusetts
- 217. Commanding General, Tank Automotive Command, Detroit Arsenal,  
Attn: J. Brooks, Centerline, Michigan
- 218. Director, U.S. Army Ballistic Research Laboratory, Attn:  
Document Library, Aberdeen Proving Ground, Maryland

219. Commanding Officer, U.S. Army Nuclear Defense Laboratory,  
Attn: Document Library, Army Chemical Center, Maryland
220. Commanding Officer and Director, U.S. Naval Radiological Defense  
Laboratory, Attn: Document Library, San Francisco, California
221. Principal Investigator, Office of Civil Defense, Contract  
OCD-OS-62-144, Research Triangle Institute, P. O. Box 490,  
Durham, North Carolina
222. Principal Investigator, Stanford Research Institute, Office of  
Civil Defense, Contract OCD-OS-62-135, 1915 University Avenue,  
Palo Alto, California
223. Armour Research Foundation of Illinois Institute of Technology,  
10 West 35th Street, Attn: C. Terrell, Chicago, Illinois
224. Brookhaven National Laboratory, Nuclear Engineering Department,  
Attn: L. P. Hatch, Upton, Long Island, New York
225. Brookhaven National Laboratory, Attn: Document Library, Upton  
Long Island, New York
226. U.S. Public Health Service, Attn: Radiological Health Division,  
Rockville, Maryland
227. Los Alamos Scientific Laboratory, Attn: Document Library, Los  
Alamos, New Mexico
228. Edgerton, Germeshausen, and Grier, Inc., Attn: Z. Gu. Burson,  
300 West Wall Street, Las Vegas, Nevada
229. Headquarters, United States Air Force, AFRDC/NU, Attn: Major  
E. Lowry, Washington, D.C.
230. Chief, Bureau of Yards and Docks, Navy Department, Attn: C-400,  
Washington, D.C.
231. North Carolina State University, Attn: W. Doggett, Chapel Hill,  
North Carolina
232. United Nuclear Corporation, 5 New Street, Attn: M. Kalos,  
White Plains, New York
233. Principal Investigator, General Dynamics/Fort Worth, Fort Worth,  
Texas
234. Principal Investigator, Technical Research Group, 2 Aerial Way,  
Syossett, New York
235. Lockheed Missiles and Space Division, Technical Information  
Center, 3251 Hanover Street, Palo Alto, California
236. Principal Investigator, Office of Civil Defense, Contract  
OCD-OS-62-14, Technical Operations Research, Burlington,  
Massachusetts
237. Principal Investigator, Office of Civil Defense, Contract  
OCD-OS-62-219, Technical Operations Research, Burlington,  
Massachusetts
238. H. E. Hungerford, Nuclear Engineering Department, Purdue  
University, Lafayette, Indiana
239. H. Goldstein, Division of Nuclear Science and Engineering,  
Columbia University, New York City, New York
240. Noel Ethridge, Ballistic Research Laboratory, Aberdeen Proving  
Ground, Aberdeen, Maryland
241. R. Aronson, Radioptics, Inc., 28 Pilgrim Avenue, Yonkers, New  
York
242. R. L. French, Radiation Research Associates, Fort Worth, Texas



- 243. M. B. Wells, Radiation Research Associates, Fort Worth, Texas
- 244. V. B. Bhanot, Physics Department, Panjab University,  
Chandigarh-3, India
- 245. Research and Development Division, AEC, ORO
- 246-889. Given distribution as shown in TID-4500 (24th ed.) under Physics  
category (75 copies - OTR)